UNIVERSITY OF STUDIES OF PADUA
DEPARTMENT OF INDUSTRIAL ENGINEERING

Master Thesis in Energy Engineering

Impact of a Guide Vane clearance Gap in a Francis turbine flow; a comparison between experimental and computational Data

Author:
Nicola Frau

Supervisor:
Giorgio Pavesi

Abroad Supervisor:
Eduard Doujak

July,14 2017

Academic Year 2016/2017

Acknowledgements

Firstly, I would like to thank my Tutor and all my TU colleagues for their availability to help me along the rugged path of my work development with willing and through useful suggestion. Then, I want to acknowledge my Supervisor for having lended me this remarkable opportunity of growth and maturation on both human and professional sides.

Contents

List of Figures

List of Tables

Abstract

The general trend of the markets nowadays and the latest government policies have promoted an increasing exploitation of renewable energies, thus their relevance on the electrical grid has experimented a rapid growth over the past years that will strengthen further in the future. Hence, this tendency has led to a dramatic increase of intermittent sources share like wind and solar power, creating deep unbalancing in the electric grid and eventually threatening the stability of the entire power system. On the other hand very little has been done to make the grid users aware towards a less irresponsibility in grid fruition, and the energy demand remains very fluctuating. In order to guarantee the service continuity, the regulation activity has thus become a central issue, involving more and more power plants, and prominently becoming the present and future core challenge in power distribution.

Hydroelectric power plants play an important role in this purpose; they, also for their large energy storage availability, are indeed able to accomplish a very fast primary and secondary regulation, therefore being the most recommended sources to face and fulfill the sudden increases on the demand. In addition to the classical turbine power plants, the necessity of a steadier demand curve and the conditions yielded by the free energy market, has led in the past decades to the pump-turbine concept development. The capability of smoothing the load curve by either acting like a pump in low demand periods or a turbine in request peaks make them a really flexible tool, precious for grid balancing.

Since hydroelectric power plants are naturally capable of this fast power adjustment, operating in efficient conditions at a wide power range becomes a central matter of concern, even more for pump-turbines power plants. This regulation is carried out in detail by the Guide Vanes section, which, by the rotation on their own shafts, regulate the flow reaching the runner and keep its inlet velocity unchanged in modulus and direction, ensuring decent work conditions even at partial loads. Nevertheless, if the exploited flow bears high sediments concentration, this section may be exposed to severe damages from erosion; whose consequences are an increasing bounded stop period, reduced of both lifetime and time between overhauls. Eventually when the geometry of the Guide Vane is heavily compromised, it brings the flow structure towards turbulence, unsteadiness, pressure and velocity pulsation, thus dropping the overall efficiency. Among the different damages, the Gap between GVs and covering plate is the most important source of wastefulness. The latter comes from a little operational Clearance planned to allow the GV regulation movement, exploited by particle laden water that, flowing through, slowly erodes and thus stretches it. The decrease in global efficiency due to GV clearance gap widening has been evaluated by most of the papers dealing with the matter around 1.5% 2% - a really relevant ratio - for high head Francis Turbines, making it a problem that deserves the most scrupulous interest.

In order to have a better understanding of this phenomenon the TU of Wien built an ex-

perimental model, that draws most of its geometry by a real machine, and was also intended to gather data for it . It is composed in a case in which is embedded a channel marked by three adjacent airfoils. Out of three, only the central one can move, adjusting angle and gap. Several measures have been taken, testing different combinations of them. The data collected feature velocities and pressure taken either in a section up and downstream of the blade.

This thesis aims to survey the effects of the Gap on the flow by replying this test rig in SolidWorks setting and then meshing and testing it, focusing the effort only on a few important cases. Given the prevailing steady nature of the phenomenon surveyed and to lighten the computational effort as well, the simulations are performed using steady state approximation. The rig is tested always at optimal open angle (set 0 in the experimental equipment) fist with Gap set to zero, to reply the simulations performed on the entire turbine, secondly the test is set to 0.2 mm to investigate the brand new operational Clearance the real turbine, and outermost 1.5 mm is considered, the wider Gap tested in the rig. Nevertheless, the 1.5 mm case is both performed in SS and transient simulation, to clarify the pulsating pressure and velocity fields in the case of most Gap vortex development. Computational Data are always validated by the experimental ones, and no considerations are performed out of the experimental context. At first are made comparisons on punctual values, trough 75 measurement per section. Then some global parameters are developed in order to provide a complete picture of the flow structure, and to have a quantitative understanding on the disturbance effects of the clearance gap vortex on the flow. The Final considerations concern the evaluation of the model reliability compared to the real situation, pointing out the flaws of the test rig and of all the test equipment in general, giving some suggestion for a potential new experimental model.

Summary

The problem of the leakage flow between Guide Vane and the covering plate due to erosion is a relevant matter and, as shown by many previous studies, a strong source of inefficiency. To investigate this issue the TU university of Wien built a model, testing it at several configurations of Gap span and closing angle of the Guide Vane. This thesis fix as goal the numerical reply and meshing of this model, in order to perform a computational reply of these tests. Then, several comparisons are made between the gathered data and the experimental ones. Those tests are performed both in Steady State and Transient mode; in particular 0 Deg of closing angle is tested with all the Gaps in Steady State, whereas in Transient one are tested 1.5 mm of Gap with 0 and 10 Degrees. The structure of the Document is now briefly illustrated:
Chapter 1 works as Introduction.
Chapter 2 starts off with a brief dissertation of the original paper than has been produced to disclose the experimental Data gathered with the Model, along with the presentation of the fundamental Data of the Turbine that had inspired the whole investigation. Then the aim of the model, along with his history are described. A detailed description of the model enclosing some pictures ends the chapter.
Chapter 3 is dedicated to the Setup arrangement: the model building in SolidWorks and the Meshing phase, including the mesh independence study are described.
Chapter 4 deals with the simulation setup in CFX-Pre, showing the settings and briefly describing the strategy applied to adjust the simulations to the different cases.
Chapter 5 describes and reviews the results gained with the simulations, both SS and Transient.
Chapter 6 collects some indications for a potential further in-depth analysis, giving some suggestions for the construction of a more detailed and reliable model.

Chapter 1

Introduction

In 2015, the energy share from renewable energies represented the 23.7% of the global electricity consumption, with the 16.6% provided by hydroelectric power plant, whereas the other renewable represent the 7.1% of the share. Unfortunately, fossil energy remains the baseload of global energy production with an output of two thirds of the total world consumption. In recent years however, renewable sources have experienced an exponential growth thanks to the awareness of the public opinion and the important investments made by the most energy-draining countries.

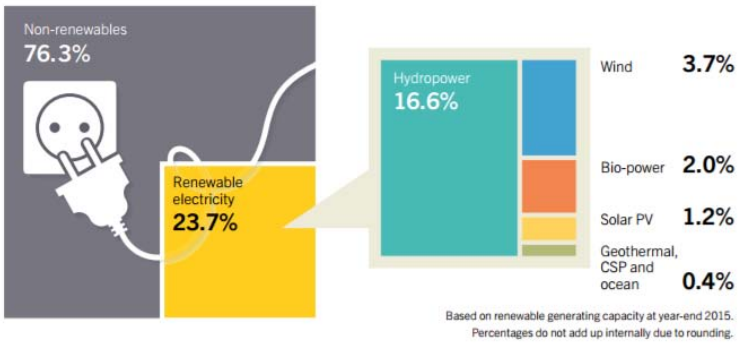

Figure 1.1: Worldwide composition of the Electric generation

Following this general Trend European Union has taken a set of commitments, drafted in 2020 climate and energy package [8] set of legislations, in which to prevent the climate change three majors goals are acquired:

- A Reduction in EU greenhouse gas emissions from 1990 levels
- Raising the share of EU energy consumption produced from renewable resources to 20%
- A 20% improvement in EUs energy efficiency

However, the stochastic nature of the most important renewable energy sources impacts the power balance on the electric grid, threatening its stability. In order to keep this balance even at

peak load conditions and to get over the issue of shifted daytime of peak power production and consumption, sufficient grid storage and fast capability of power regulation has to be provided. While fossil sources have hardly adaptable attitudes to peak load fulfillment and quick power control, hydroelectric power plants play an important role in this purpose. With their large energy storage availability, they are indeed able to accomplish a very fast primary and secondary regulation, therefore being the most recommended sources to face and fulfill the sudden increases on the power demand.

Historical context: The hydroelectric energy is one of the most ancient sources of power that man has ever harnessed. It has kept his preeminent position even at the beginning of the second industrial revolution, as the idea of using the water power for electrical conversion has begun to arise, becoming eventually one of the biggest power sources for humanity. Hydroelectric has several merits, such as being renewable, high concentration of power and capability of fast regulation. This latter skill has led to the exploitation of the machines in a wider range of operational loads, causing stress problems in machines suited for working mostly at design conditions. Problems at high dynamic load are raised as well as vibration issues in rotor-stator interaction. Moreover long-periods-stress periodicity has to be considered, such as start and stop cycles.

1.1 Francis Turbines

Among the water power exploitation machines, Francis Turbine figures as the most commonly used. This machine is common for medium flow rate and head situations. It is classified as a reaction machine, which converts both kinetic and pressure energies into a mechanical output. The machine features several components, each absolving peculiar requirements:

- Spiral Casing: It gathers the water, conveying it throughout the circular set of the Stay Vanes section. It has to be designed to provide uniform amount of fluid in every circular span, thus its section needs to be decreasing. Usually is built by some conical sections welded together.

- Stay Vanes Section: This section is the first the water encounters after draft tube, it features welded stay vanes and, since is made only for structure consolidating purposes, the number of them is reduced to the smallest possible. The blades are thus made to have the minimal affection on the flow, therefore designed to follow the free flow path of the water.

- Guide Vanes: Movable vanes entrusted with the regulation of water modulus and direction. They have the primary function of conversion of pressure to kinetic energy. A through shaft acts in every GV both as center of rotation and supporting element and is moved together with the others by a unique servo-motor, that regulates the angle of attachment according to the required load variations. The GVs regulate indeed the water flow to keep the inlet angle almost constant at load variation, thus avoiding the water impingement on the runner inlet blade, keeping the efficiency at the best possible level. They also act as flow interrupting tools, since by reducing the angle they can overlap each other and completely stop the flow in the runner.

- Runner: This is the core of the machine, it converts both kinetic and pressure energy in mechanical one, available at the shaft. In this component the flow enters in radial direction, is right away processed by the runner blades, and then drained axial wise.

- Draft Tube: Divergent duct downstream of the runner that conveys water to the lower basin. It is usually bent in right angle towards the final drain.

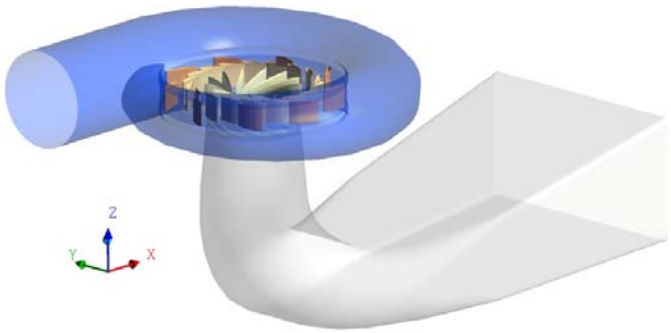

Figure 1.2: Depiction of a Francis Turbine

The Guide Vanes section, which is the most important statoric part of the turbine, helps to convert some pressure energy in kinetic before the encounter with the runner. Moreover the GVs can be moved, all at once, to adjust the flow field and to regulate the flow rate towards the most efficient configuration. Besides Francis turbines are pretty sensitive to load conditions, and they tend to undergo severe efficiency drop when employed at partial load.
Ending up, every turbine is built with a certain gap between the guide vane and the head cover, to prevent the components from grinding. The decrease in global efficiency due to GV clearance gap widening has been evaluated by most of the papers dealing with the matter around 1.5% / 2% - a really relevant ratio - for high head Francis Turbines, making it a problem that deserves the most scrupulous interest. So this Gap will be the core of our analysis.

1.2 GV operational Gap

The GV operational Gap can vary, at dry design conditions, from 0.1 to 0.3 millimeters depending on the machines. Nevertheless once the turbine is operating, the pressurized internal channel makes both bottom and head cover warp slightly, eventually increasing the gap. Therefore water, wedging into this split, gives rise to a secondary flow that disturb the overall pressure and velocity fields with pulsating phenomena and velocity deflection. The cross flow depends strongly by pressure gradients between GVs pressure and suction sides, that are yet needful in order to set an uniform flow for the runner inlet, and turn up roughly from the middle of the chord span to the aft part, coming out eventually as a vortex arising in the airfoil rears suction side. The general result is an overall deflection of the velocity by heightening the runner inlet angle; therefore it leads to a loss of theoretical efficiency by decreasing its tangential component, according to Eulers rule ($\eta = u_1 c_{u1} - u_2 c_{u2}$). It consequently increases the absolute value of the relative velocity, with an enhancement of friction losses and erosion phenomena on the runner blades. Moreover, if the flow carries sediment particles, it may start a process of progressive erosion of both GV and covering plates, further heavily concerning the surfaces near to the leakage vortex extension. If this process starts, it is widely supported by the unsteady and pulsating nature of the vortex, and in time it carves the surfaces in a rough and uneven pattern, due to the stochastic nature of both particle size and the turbulence phenomenon, deeply modifying the GV profile. These wear phenomena boost the cross flow instability even more, and eventually this vicious cycle brings

to the total impracticability of the entire machine and its forced shutdown.
Erosion is a common issue for all the hydraulic power plants to deal with, but it especially affects high head machines, such as Pelton and Francis turbines, because of the high velocities involved, occurring in the most sensitive components.

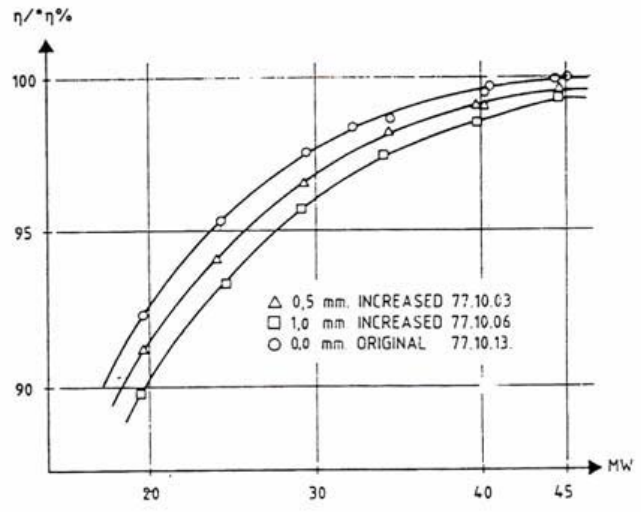

Figure 1.3: Efficiency drop graphic taken by the case disclosed in [14] ; it shows how relevant is the phenomenon

1.3 The problem of the Wear in Turbines

Since the beginning of the exploitation of hydroelectric energy the problem of the erosion and the damage to the hydroelectric equipment has been very commonly experimented, especially in plants that exploit basins, in which usually Francis or Pelton turbines are installed. This issue, occurring in the most important components, brings usually to vibration and variations of the flow paths, scaling the inefficient ones up, and may even end up in final breakdown of the machine. Erosion is caused by sediment particles collected by the rivers along their path and carried towards basins, in which the finer ones are kept suspended and end up to be conveyed in the machines. Erosion rate, as it will be explained later, depends upon size material and concentration of the particles, so although the consequences are experienced in the majority of the power plants, the turbines are affected by the characteristics of the raw materials carried by the river and the general seasonal trend. As a matter of facts, the steep increase of the flow rate, experienced in the good season months and led by the natural process of snow melting, brings along the sediment trapped inside the ices and furthermore those collected alongside the mountains creeks. Hence, if we take the GV Gap Widening as benchmark, while in the Alps wear occurs in a moderate way, resulting in maximum gaps of 1-1.5 mm, in different places such Andes and Himalaya, complicit the longer rivers and the concentration of the seasonal precipitations, the gap can reach even 3-4 mm. Many quoted paper treating Nepal power plants [12] claim that in the last decades the demanded power has experienced a continuous growth, forcing the exploitation of high content particle sources as well. The documents also speak about of power

plant forced stops right at the maximum production potentiality, in order to prevent irreparable damages to the equipment. Thus it seems that most of turbines suffer from wear and erosion phenomena, which, as widely discussed in all the documentation, either come to the degradation of power plant performance, the reduction of equipment lifetime and to the increase bounded stop periods for overhauls and repair requirements. Moreover the erosion cause a turbulence enhancement, and since the particle motion is governed by the local flow patterns, wear mechanism feed itself, finally leading to a relevant flow disturbance that may eventually come out as an overall efficiency drop. Since the focus is on Francis turbines, the attention will be shrunk on the high head ones indeed operating with water at high sediment content, exposed as they are at higher velocities, accelerations and pressure gradients.

In the following paragraphs we will briefly introduce the erosion mechanisms, how to forecast the damages and finally give some general suggestions to prevent both of them.

1.3.1 Erosive Wear

Erosive wear is affected by several factors which regulate erosion rate. The main elements that affect the phenomenon are:

1. Operating Conditions: velocity, acceleration, impingement angle, flux rate or concentration, medium of flow and temperature.
2. Eroding particles properties: size, shape and hardness of the material
3. Target material properties: physical, such as elasticity and hardness, and chemical properties, like surface morphology.

However the most important factors remain velocity, impingement angle and particle concentration, since we they can be found in every eroding situation.
Several studies have been conducted to have a better understanding of the airfoil leakage phenomenon [7, 24]. Unfortunately to study this phenomenon is a very complicated matter, because under a long time erosion the gap span is strongly uneven, impossible to foresee and describe in detail. The only conclusion made by the most of the studies is that this raugh gap boosts the turbulence advantaging the mixing and settlement of the velocity profile.

1.3.2 Erosion Categorisation

There are different types of erosion mechanisms, Duan and Karelin classify them in three categories:

- Micro Erosion: caused by small particles ($d < 60\ \mu m$) exposed at high rotational velocities due to the turbulence in the boundary layer, thus inducing abrasive erosion most likely at high turbulence regions (Trailing edge).
- Secondary flow erosion: caused by the particles snared in the horseshoe vortices rising from the interaction of the flow and the GV and generally around obstacles. This type of erosion is a combination of Boundary Layer effect and and change of flow acceleration.
- Acceleration of high diameter particles ($d < 0.5\ mm$), that end up to proceed normal to the streamline and collide with the wall.

Bardal presents another sorting of erosion categories, similar to the previous one:

- Impingement erosion: occurs when a particle laden flow undergo a deviation in the flow direction until collides with the surface.
- Turbulence erosion: It happens in high acceleration zones of the flow.
- Wear and Tear due to particles flowing along and in contact with the surface.

1.3.3 Erosion Models

Erosion rate is correlated to several features including the material, velocity of the flow and concentration of particles in it. According to Truscott and many others authors several models have been built to point out the dependence between erosion and velocity. All the papers based on the experimental data agree to a dependence by the velocity with exponent depending on the material type, but in any case near to three. In the matter of the dependence by particle content all the models tend to converge at a linear function. A model disclosed in [34] is hereby presented as example:

$$W = K_{mat}\ K_{env}\ c\ V^{i}\ f(\alpha)$$

Where the erosion rate, W, is given as $mm/year$. K_{mat} is the material constant, K_{env} is the constant describing the environment, c s the concentration of particles and $f(\alpha)$ is a function of impingement angle. Other models take more variables into account such as Tabakoff's model and Bergeron's model.

1.3.4 Mechanism of erosion in the Guide Vanes

Even the GV section is characterized by its own main causes of erosion:

- Turbulence erosion: Occurs both on facing plates and GV in the rear part of the GV ring; arises from the profile turbulent wake.
- Secondary flow erosion: occurs in corners like between the facing plate and the GV, is caused by the horseshoe vortices around obstacles like GV.
- Leakage Erosion: The flow leaks through the operational Gap between GV and facing plates undergoing steep accelerations.

1.3.5 Methods of erosion forecast and outmost erosion zones

In order to foresee the wear behavior finite volume analysis have been performed, based on the calculation of several individual sand particle paths across the flow field, the so-called Lagrangian tracking, using those resultant paths to describe the average behaviour of the whole dispersed phase, the particle laden flow indeed. It is essential to stress out that before undertaking those calculation, the flow field of predominant phase needs to be solved. By varying the parameters related to particle nature (size, material) and combining the displayed paths with the suitable Erosion Model, detailed erosion forecastings are provided. All the papers agree in general terms on the places of prevailing wear, as follows:

- The forward part (nose) of the Guide Vane, reached by heavier particles.
- The rear part of the suction side, in which acts the leakage vortex development, establishing a high turbulence zone that support erosion.
- The regions of the covering plates nearby the latter one, damaged by the same mechanism.

1.3.6 Suggestions

In order to prevent wear some measures can be adopted at design stage as well as in mending phases during overhauls. Here are shown some of them:

1. *Increased turbine diameter:*
   - Advantages: Reduction of relative velocity, hence reduced erosion.
   - Disadvantages: Increased material cost and space requirements.
2. *Thicker runner blades:*
   - Advantages: Increased time before structural damages.
   - Disadvantages: Decreased efficiency and increased risk of vibrations, caused by Von Karman vortices.
3. *Fewer runner blades:*
   - Advantages: improved access to the flow channel for coating purposes.
   - Disadvantages: May result in reduced cavitation performance.
4. *Coating on exposed parts:*
   - Advantages: Increased abrasion resistance on the surface.
   - Disadvantages: May increase surface roughness, which may reduce the efficiency. Increased production cost.

1.4 Background

As pointed out in the introduction, although leakage flow is a really remarkable problem, actually few studies have been performed in this direction. Among them, several strategies have been employed to highlight the flow structure better. The most covered one is a comparison between experimental data gained from a test rig and the simultaneous CFD Testing. The models can be distinguished in 2D and 3D ones. The principal issue of the 3D models is reproducing reliable flow conditions at GV inlet. Infact the following passages through the funneling pipes and the draft tube creates different secondary flows that, even faded and softened by the passage in the stator vane, continue to have their influence. So different strategies to overcome this problem and to have a more realistic simulation have been tried: from an initial entrance section, shaped following the free vortex law up to the simulation of the entire draft tube segment. Actually most of the studies focus on the overall effect, considering the efficiency drop in presence of erosion of all components, without surveying in detail the flow structure modification due only to leakage Gap. The same ones usually report efficiency comparisons related to turbines earlier affected by this issue and then mended using sealing strips and coating remedies on the components. Others

focus, by the realisation of reliable models, on the description of the flow structure, providing valuable visualisations of pressure and velocity fields to isolate and display the leakage vortex. However, many of them treat a partial view of the phenomenon, so the picture returned from this studies ensue to be quite fragmentary. Some, like mentioned before, are focused directly on experimental efficiency drop limiting themselves to a superficial describing of the other features implied while some others highlight the flow field structure in detail, but without bringing any quantifiable parameter to take in account the alteration in fluid structure arising with the presence of the gap. Some other focus mainly on erosion prediction models and identify the weakest areas eventually recommending a material strengthening of those zone. Unfortunately, as a matter of facts none of them gives a parameter that can quantitatively take to account the worsening effects of the vortex, as conversely it will be tried in this work.

Some papers will be contextually quoted: they will be briefly described illustrating main areas of interest and purposes of each. The most important ones will be summarized, in order to give a better idea of the background from which this Thesis takes the start.

1. S. Chitrakar, B. Singh Thapa, O.G. Dahlhaug, H.Prasad Neopane, *Numerical investigation of the flow phenomena around a low specific speed Francis turbine s guide vane cascade* : This paper investigates the flow phenomena around the guide vane cascade through a real model and computational techniques employing 3 different turbulence models. The speed distribution obtained are compared with experimental data in graphics, both at GV outlet and runner inlet. The influence of clearance Gap increasing on the flow is studied, demonstrating how the pressure gradient between suction and pressure side affects the leakage flow, and hence how this reduction would decrease pressure pulsation and erosion rate. The paper also shows how all the velocity gradients (foil wake effect, gap vortex) soften in experimental data compared to the simulated fields, like it will be in our case.

2. R. Koirala, B. Zhu, H. Prasad Neopane, *Effect of guide vane clearance gap on a Francis turbine performance* : This paper starts with the observation of the severity of the effects in hydropower plants of clearance gaps on general performance, achieved through computational methods. Some picture of damaged GVs along with erosion prediction graphics are presented. The principal section of the paper proposes an empirical method to estimate leakage flow through the Gap. This equation is presented by several papers, and will be also employed in this work. The formula is then validated with both experimental and computational data, with excellent results and the smallest discrepancies. The paper conclusion is marked by several pictures of tangential streamlines at leading and trailing edge, showing the leakage vortex development.

3. S. Eide, H. Brekke, *Analysis of the head covers deflection and the leakage flow in the guide vanes*: This paper focuses on a different issue compared to the previous ones: whereas in those the erosion is the main cause of the gap presence, hereby is presented a different cause: the head cover deflection due to high pressure of the inlet sections. A 2D simulation of 20 pressurized head covers is introduced, that is further validated with the 3D simulations of the same component. Then the influence of the erosion in gap stretching in recognized and some efficiency graphics with and without erosion are presented, along with efficiency plotted against the head cover stiffness, deflection and Reynolds number of the leakage flow. The paper concludes considering that the efficiency is highly influenced by the extent of the clearance gap, and finally presenting some vectorial depiction of the flow in the gap.

4. S. Eide, O. G. Dahlhaug, *Analysis of the leakage flow and wear in guide vanes* : This paper centers on the efficiency drop due to erosion. To do so, a 2D simulation of a pressurized

head cover is introduced, to calculate the pressure distribution and then get to the cover deflection. The measurements show also the importance of reducing the wear possibilities from a design point of view and also the importance of repairing any onset of erosion. Finally, some plots of efficiency against flow at different clearance gaps are presented.

5. W. Liao, J. Li, *Numerical simulation and experimental investigation of the flow in end clearance region of the Guide-Vane row of hydraulic turbine* : This essay presents the influence of leakage flow on the main one and the spreading of the so created vortex towards the runner inlet. It features also pressure distribution measurements along the chord span, at different heights and in both no gap and gap conditions. Then two types of guide vanes are compared, the standard solid type and a hollow one, demonstrating how the sudden step provided by the hollow configuration helps the attenuation of pressure gradient, along with the leakage flow entity. The paper ends with the presentation of several vector and streamline plots, to display the leakage and the rear vortex rising at high closing angles.

6. B. S. Thapa, O. G. Dahlhaug, B. Thapa, *Velocity and pressure measurements in guide vane clearance gap of a low specific speed Francis turbine* : This essay employs a model of three blades. It focuses on pressure and velocity measurements, introducing a thorough description of runner inlet velocity distribution. It can be seen that the leakage flow causes a steep increasing of normal part of the velocity in the regions interested by the leakage vortex, that worsen the overall performance according to Euler turbine equation. Then it is shown, also by pictures, how it leads to unstable pressure and velocity distributions, enhancing erosion on both guide vane and runner blades.

7. R. Mack, P. Drtina, E. Lang, *Numerical prediction of erosion on guide vanes and in labyrinth seals in hydraulic turbines*: Centers on the wear mechanisms, predicting where the erosion should occur the most, by making comparisons between a real model and a CFD reply simulations on a 3 blade mode, including the shafts and circular inlet and outlet sections. At the end a prediction of the vortex core development is presented, and the influence of the turbulence enhancement contribute to an erosion improvement.

1.5 Thesis Objective

The main objective of the thesis is to examine the flow structure in the GV section under Gap leakage flow. The needing, besides being a core problem during the machine maintenance, comes in this very case from some measurements conducted in a real machine, whose Data will be later presented. In order to set a proper experiment and to reduce the further computational effort a little periodic element is isolated, including 2 completed GV flow channels. Then, because of the steady availability of the Data, a preexisting model has been exploited, that quite replies the geometry of the isolated section. The model tests were performed using air as fluid, so the computational side has be carried out employing air too.
This thesis aims to survey the effects of the Gap on the flow by recreating this test rig in SolidWorks setting and testing it, focusing the effort on three important cases only. Given the prevailing steady nature of the phenomenon surveyed and to lighten the computational effort, the simulations are performed using steady state approximation. The rig is always tested at optimal open angle (set 0 Deg in the experimental equipment) fist with Gap set to zero, in order to reply the simulations performed on the entire turbine, secondly the test is set to 0.2 mm to investigate the brand new operational Clearance of the real turbine, and outermost 1.5 mm is considered, the wider Gap tested in the rig. Nevertheless, the 1.5 mm case is both performed in SS and

transient simulation, to clarify the pulsating pressure and velocity fields in the case of most Gap vortex development. Computational Data are always validated by the experimental ones, and no considerations are performed out of the experimental context. If the results are validated by the experimental ones among a reasonable error percentage, the simulated model will be used for further studies on the wake near the trailing edge and on the leakage flow between pressure and suction side.

At first comparisons are made on punctual values, trough 75 measurement points per section. Then some global parameters are developed in order to supply a complete picture of the flow structure, and to have a quantitative understanding on the disturbance effects of the clearance gap vortex on the flow. This thesis will also attempt to give a parameter that can quantitatively take in account the worsening effects of the vortex on the overall efficiency. Different computational models will be employed in order to supply a clearer view of the phenomenon.

1.6 Document Structure

The document is divided in chapters. This Chapter fulfills the task to introduce the matter giving also a general portraying of the context and then focusing on the thesis argument.

- Chapter 2 starts with a brief dissertation of the paper that has been produced to investigate on the experimental Data gathered with the Model, along with the presentation of the fundamental Data of the Turbine that had inspired the whole investigation. Then the aim of the model, along with its history are described. A detailed description of the model enclosing some pictures ends the chapter.
- Chapter 3 is dedicated to the Setup arrangement: the model building in SolidWorks and the Meshing phase, including the mesh independence study are described.
- Chapter 4 deals with the simulation setup in CFX-Pre, introducing the settings and briefly describing the strategy applied to adjust the simulations to the different cases.
- Chapter 5 discloses the results and provides a critical comment
- Chapter 6 collects some suggestions for an eventual further work

Chapter 2

The employed Model

In order to investigate the leakage flow phenomenon deeper, brought to attention by the observation of the real machine guide vanes, it has been built an acrylic model that features 2 entire Guide Vane channels. In this chapter this model will be described in close detail, starting by the Paper issued after some test were performed on it.

2.1 Original Paper Description

2.1.1 Data of the turbine

The Power Plant on which the Paper and the model are based, has a Francis Turbine that features the following Data:

$$H = 672\ m$$

$$Q = 9.81\ m^3/s$$

$$P = 79400\ HP$$

$$k = 0.336237$$

$$n_s = 17.79$$

The model doesn t reply the machine portion exactly, making some changes in order to allow an easier construction and employment.

2.1.2 The Paper

The Paper [1] is so structurated:

Title: *Analyse der Strmung und der Verluste im Leitschaufelbereich von Francisturbinen*
It describes the leakage flow putting the accent on the improvement of the efficiency due to the introduction some sealing strips, but the main goal is the presentation of the results gained with the built test rig, presented in the last section.

Chapter Description:

- Chapter 1: General focusing of the matter, followed by a brief description of the document structure and completed by a discussion on the historical frame and state of the art context.

- Chapter 2: Some Literature studies are presented. First a general description of the standard interaction between a vane and the flow is disclosed, pointing out the vortices arising at full capacity, and excluding the presence of the Gap: the horseshoe vortex, the corner vortex and the suction side vortex. All these secondary flows are described and depicted with some explanation images. Then the gap vortex and its influence is described in close detail: several pressure graphics plotted along the airfoil profile are presented, together with an accurate explanation of the different gap regions in which different type flow develops. The following section is dedicated to a presentation, based on literature [14], of the efficiency drop under erosion, along with a complete graphic of normalized efficiency versus mass flow rate with and without erosion. Three different machines are considered, and it can be seen that the efficiency drop is quite important, and more relevant in high head Francis turbines. As predicted, the drop is more significant at partial loads, far from the optimal point. In one of the cases the efficiency plot is presented with and without some sealing strips, bringing out the matter of turbine mending, and showing a relevant improvement in the performances. Then an important model followed by the complete set of results is presented. The model is composed in a entry pipe that approach tangentially (as a real machine does) to a set of five stay vanes followed by five GV; than the drain section gathers the flow downstream. A pressure plot in the between of the guide vane is provided, along with others highlighting the SV-GV interaction. Then some graphics are presented for pressure plots alongside the GV, and field plot in the section of the gap between GV and the facing plate.

- Chapter 3: The third chapter deals with the description of the actual model and the rest of the experimental setup. The test is carried out using a fan that blows air into a convergent conduct, to accelerate and stabilize the flow, then entering the model. A more detailed descriprion of the latter will be provided further in this Chapter.

- Chapter 4 features a theoretical approach for the determination of the power loss related to leakage flow. In order to do that, a set of intermediate parameters is presented; the effort is headed towards the determination of pressure difference between pressure and suction side and leaking flow rate. All the dissertations are taken from the document *Experimentelle Untersuchungen an axial durchstromten Ringspalten* by Stampa, Burkhard; Dissertation; Technische Universitat Braunschweig; 1968 document.

- Chapter 5: Conclusion and final acknowledgement of the writers to their sources. It also feature a brief description of the document structure.

Presentation of the results: Then all the results are presented. They at first features the entire flow field for all the gaps but only for angles from 0 to 6 Degrees. Two tridimensional graphics are presented, one for the ratio v/v_{inlet} and the other for the bidimensional angle in the $x-y$ plane positive in y direction. Then the two equivalent bidimensional graphics, parametrized in height z, are depicted, together with a 2D disclosure of the flow field. The results are presented with no comments. The cases surveyed corresponds to the combinations between $[0; 0.2; 0.4; 0.6; 0.8; 1; 1.5]$ mm of gap and the angles $[0; 2; 4; 6]$ deg. Later it will be tried to make a comparison on the same plot between the experimental data and the computational ones.

2.2 General Description

This model helps to understand the flow behaviour under a certain erosion degree of the guide vane, that brings to the creation of a gap between the case and the GV. It replies a portion of the GV section enclosing two entire GV channels, trimmed by the adjacent profiles and by some walls. Instead of water, the model employs air as test fluid, supplied upstream by an air blower. This choice has been taken for different reasons: an air supply is indeed easier to set up and control, it is for instance less serious and more manageable to neglect the small leaks and constructional issues in the experimental equipment. Most importantly, the model doesn t need to be built to face the high dynamical thrust whom the water employment would have led to, it allows to use cheaper material and to pay less attention in the model construction phase. Hence, it has been used acrylic as material, that with its transparency allows PIV methods of measurement. Furthermore with the same power consumption a water model would have been far smaller. The experimental data collected, given the different physical properties of the fluids, are comparable but not exactly corresponding to the real situation. However, the main issue related to the different nature of the two fluids is absent: the air flowing with a velocity in full subsonic range doesn' t show relevant density variation (Role of Mach number), it can be considered a nearly incompressible fluid, that makes it ultimately a good substitute for water.

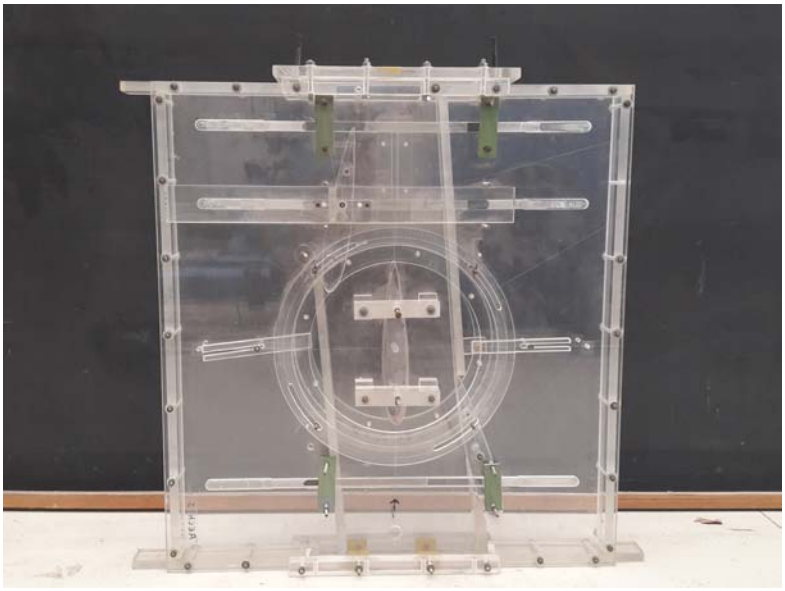

Figure 2.1: The model: Inlet section is located downside, Outlet section upside. Ceiling section, with its hole for the rotational part, is placed on the front side while floor section is behind

The model isolates a nearly straight channel built around an adjustable airfoil, featuring also the the other two nearest ones. Instead of studying the flow behaviour between two adjacent blades this model focuses mostly on the wake development, setting up two measurement sections downstream the blade. The angle formed by the chord direction and the circumference in which the blades rotation centers are placed is at first 30 degrees, aligned with the direction of the incoming flow.
Starting from this initial position whereby the angle parameter Beta (β) is considered zero, other

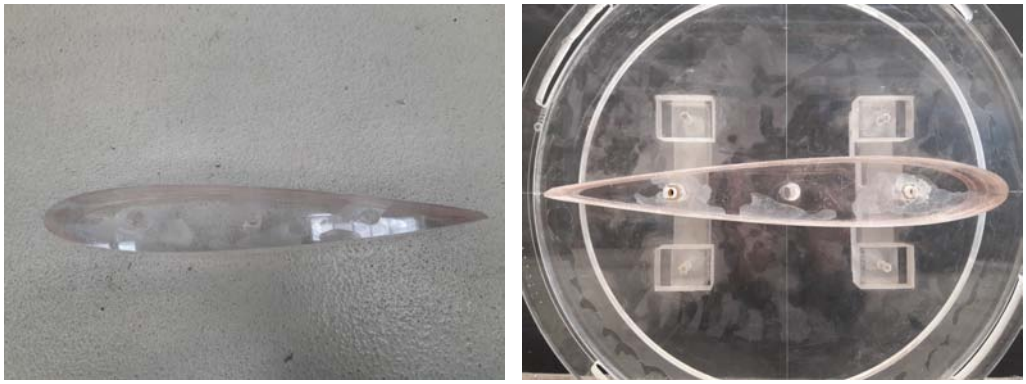

(a) The detail of the Airfoil (b) The whole rotational Mechanism

Figure 2.2: Model components

tests are performed at several angles, checking the airblade both at progressive closing positions and different gaps.

2.3 Detailed Description

The model presents as rectangular shaped body, with similar height and width (nearly a square surface) and a smaller depth. It is built in acrylic, a pretty hardy material, which besides allows to see directly the flow field during the experiment, and its assembled using glue and screws. The model simulates a portion of an existing guide vane section, which consists in 24 NACA 3000 profiles, featuring only 3 of them, placed in the respective positions of the real ones. The model includes only three of them, conveniently harnessed into a wall system.
Whereas the two side ones are fixed, kept in positions by screws, the central one, as said earlier, can move in two different modalities. In addition, several walls are placed to create a channel that embodies the 2 side stator blades, in which the stream is supposed to flow. A couple of nearly square walls closes up the model, finally shaping the channel in its final form. These two sections will be called *Floor* and *Ceiling* from now on, since this is what in those positions looks like. In the ceiling section is applied a circular hole, of 300 mm of diameter, to allow the central profile rotation, filled up with a thin disc, cut in the center in airfoils shape. The hole has to be filled with the airfoil, completing the handling mechanism useful for the experiment. The thickness of the walls is 15 mm while the channel height is of 50 mm. After quickly describing the model s shape it can be pointed out the existence of two free surfaces, that will be the *Inlet* and the *Outlet* section. The model features an inlet and a narrower outlet section, and in general all the channel shape shrinks gradually, causing an overall acceleration of the flow. Moreover in the left side the orientation of the blade brings to a fast constriction of the channel, forcing the flow to react assuming trajectories issued by the blade shape. All the mentioned sections are described in Figure 2.1

The central airfoil as it has been said earlier, can be moved in two ways, it can rotate around a centre placed at 131 mm from the nose in the chord path and it can be moved up and down in the GV axial direction. These two degrees of freedom allow to control the angle β and the gap s. According to the variation of those parameters all the different tests are performed. Whereas

with the tests at different angles several load condition are simulated, the gap is needed to take the erosion into account.

2.3.1 Measurement Section and Data Avaliability

Three different measurement sections are considered, placed in three relevant position according to the flow development. The first one, called *Inlet* and is placed right after the inlet. It measures the velocity at the entrance of the model, which has not been affected by the central blade yet. The other sections are positioned in the rear part of the model; the first helps to understand the vorticity and the velocity distribution soon downstream among the airfoil; the second is located closely to the outlet, right at the trailing edge of the left airfoil, showing how the flow flows (how much vorticity drops) just before enter the rotor blades. All the sections present 15 rows of points spaced by 10 mm one of each other. Each row includes 5 measurement points. The measurement tool is a two-wires anemometer, set to measure only x and y directions. So z component, along with a complete depiction of the vortex structure are not taken in account.
Those mentioned 75 points gather the module and the angle of the velocity. Unfortunately among all the measurements previously collected a few part has been lost, thus only data related to the inlet and first section are available.

The data gathered are:

1. Module of the velocity projection on xy plane on the measurement Section 1
2. Angle of inclination on y direction, counted from x axis positive in y direction, in the same section
3. The velocity modulus of inlet section
4. The ratio between velocities at 1 and inlet Sections
5. The relative pressure
6. Data of the first and second wire, then employed to calculate the velocity
7. Temperature of the downstream section

All these data for every measurement point.

Model measures and references:
Regarding the point lying on the inlet section, belonging to floor plane and resultant from the intersection with the elongation of the chord axis as the origin we can state: Referring to the lifted model, laying on its inlet section: Model height: 847 mm Model width (case): . Distance from the inlet of: Inlet Section= 155 mm 1st section of measurement: 649 mm 2nd section of measurement: 772 mm

Inlet width: 278 mm Outlet width: 169 mm

Measurement Tool
Two wire anemometer: every wire is heated at kept at constant temperature. This tool resting on the exchange process on the wire, detects the velocity component towards its orientation axis, so properly orientated this tool has detected x and y components of the velocity. Unfortunately,

no measurements on z axis have been performed, so the vortex structure cant properly be highlighted. Since the location of the anemometer is different from the measure place due to its overall dimension, the real measurement sections are 3 mm upper in z direction.

Chapter 3

Setup Arrangement

3.1 SolidWorks Building

The model has been accurately measured and then faithfully replied using the software SolidWorks. For the airfoil, the paper indicates the proper NACA type but the chord length is different from model to paper. So, an empirical and measuring approach is preferred for the airfoil shape as well. Furthermore, given the lack of measurement instruments, the profile has been gained through a program that converts drawn sketches in a table of points. The curve then is imported in SW workspace. The reply is then completed by embedding the three so gotten GVs in the other walls considered. Since it is aimed to the tightest possible representation of the real model, its fictional representation has been built resting first on personal measurements rather than the report declared dimensions. The model is at first built in three separate part files, that for convenience we call *Airfoil, Wall* and *Rotational Part*, and then assembled in a overall Assembly Document file.

3.2 Meshing Considerations

3.2.1 Mesh building Strategies

For the Meshing part ICEM CFD software has been used. Because of the foreseen complexity of the flow structure, a structured mesh will be employed instead of an unstructured one. This increases the precision of the solution especially in the gap and rear areas, where elements stretched in the same direction of the flow helps to keep the error propagation under a reasonable threshold. A good grid is indeed essential to achieve credible results, since the choice of properties will affect the accuracy and convergence of the solution. The governing equations for the physics in fluid domain are based on the principles of Newton's 2nd law, mass and energy conservation. Measures of mesh orthogonality, expansion and aspect ratio are generally used as significant measures for mesh quality. The limitations included in the solver was used as reference. It is important to realize that the measures are intimately related to the solver used and values heavily depend on the discretisation method. In order to provide a solution indipendent from the meshing, a Mesh Independence Study has been performed.

3.2.2 Turbulence Models

The most exploited model at industrial level is $k - \epsilon$, that guarantees numerical robustness in fully developed or rather free stream flow. Conversely it is not valid for flow in high pressure and velocity gradients, such as near to boundary layer, in curved surfaces or dealing with rotating fluids. In this simulation the boundary layer calculations become central (dealing with a gaps of a few tenths of millimeter); there are also several regions in which the wall undergoes high bending, so in order to achieve accurate results in these zone a $k-\omega$ model has to be employed. This model has a high reliability rate in the viscous sublayer, but it requires a heavier computational effort. Since the mesh presents both situation, the Shear-Stress-Transport model has been employed. This, resting on an automatic wall function, applies $k - \omega$ model near the walls and $k - \epsilon$ in the free stream region, blending the two models in the connecting zones. Speaking in general terms, for all CFD models a fine grid resolution is required close to the walls in order to get a reliable solution for the boundary layer. The ratio on which the mesh quality near the wall can be judged is a non dimensional wall distance, that is hereby defined like:

$$y^+ = \frac{u_t \; y}{\nu}$$

Where ut is the friction velocity at the nearest wall, defined as $\sqrt{\tau_w/\rho}$ (τ_w is the friction force), y is the distance of the nearest node to the wall, and ν is the local kinematic viscosity. Different turbulence models have different y^+ requirements, the SST model needs $y^+ < 5 - 8$ to produce convergent results.

3.2.3 Mesh description

The mesh area is approximately rectangular-shaped, interrupted in its extent by the GV volume. So the strategy employed is now visualized:

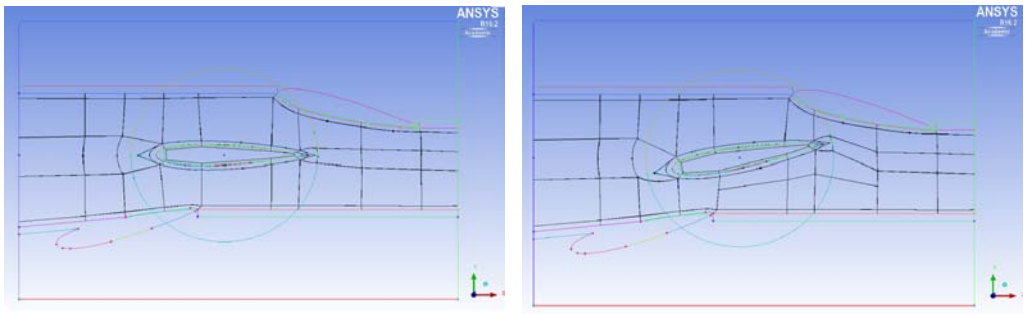

(a) Blocking Displacement under 0 Degrees condition

(b) Blocking Displacement under 10 Degrees condition

Figure 3.1: Blocking displacement and organisation

As can be seen in the image above, the longitudinal span, from inlet to outlet, is divided in three different rows of blocks, with additional slender blocks to mark and treat separately the boundary layer. The central row contains the profile, which is meshed separately using the external O-grid tool on the polygonal outline assigned to the profile contour. An additional block

is arranged right at the rear of the profile, in order to have a thicker element region where it is forecasted an instability zone. The length of the channel is marked by 9 consecutive stages of blocks, in order to have both a Mesh fine and elastic enough to fullfill the accurancy requirements. The Gap is meshed through an internal O-grid, while the gap span is discretised in series of blocks of 10 elements for the smallest and 15 for the widest ones.
For the high closing angles of the profile the mesh strategy presents an unique difference: since the wake on the suction side becomes turbulent and there the flow field become unstable, other 3 blocks are added in the longitudinal direction in order to heighten the concentration on the zone of foreseen develop of the vortex.

3.3 Mesh Independence Study

The solution of numerical models depends always upon the solver grid. If computational resources allow it, it is always recommended to adapt the grid until the solution is independent of the mesh. When grid independence is obtained, the coursest independent mesh should be used in further analyses to save computational resources.
Consequently, in order to study the independence of the data to the mesh it has been followed the Grid Convergence Method (GCI), based on Richardson studies, first exhibited in [4], as described in [2]. The quality of a meshing strategy can be perceived by the stability of some reference values calculated in three meshes, with the same geometry but with different number of elements.

The Richardson method indeed implies to take in account three different meshes, in an increasing finer scale. Every mesh is characterized by an adimensional parameter, h, which represents the medium extent of its elements through an equivalent length dimension and is defined as:

$$h = \left[\frac{1}{N} \sum_{i=1}^{N} (\Delta V_i) \right]^{1/3}$$

Consequently:

$$h_1 < h_2 < h_3$$

Where pedix 1 stands for the finest mesh. Then, the document makes the following definitions:

$$r_{21} = h_2/h_1$$
$$r_{32} = h_3/h_2$$

According to the document, in order to survey only three meshes, instead of 5 or more as the previous methods were predicting, the ratio between the parameters of two subsequent meshes has to be greater than 1,3 . The document s main aim is to provide a procedure for estimation of the error correlated to the domain discretization, and also to give a quantitative measurement of the quality of the convergence ratio and a way to calculate a target value, reached only theoretically by a mesh with an infinite number of elements, to whom the same other three taken in consideration, calculated by the three meshes, refer to.
Then, the document [2] employes those values, referred as ϕ , to enstablish some parameters:

$$\epsilon_{21} = \phi_2 - \phi_1$$

$$s = sgn(\epsilon_{32}/\epsilon_{21})$$
$$q(p) = ln\left(\frac{{r_{21}}^p - s}{{r_{32}}^p - s}\right)$$
$$p = \frac{1}{ln(r_{21})}|ln|\epsilon_{32}/\epsilon_{21}| + q(p)|$$

Now, having evaluated the the exponent p iteratively:

$${\phi_{ext}}^{21} = \frac{{r_{21}}^p \phi_1 - \phi_2}{{r_{21}}^p - 1}$$

$${e_a}^{21} = \left|\frac{\phi_1 - \phi_2}{\phi_1}\right|$$

$${e_{ext}}^{21} = \left|\frac{{\phi_{ext}}^{12} - \phi_1}{\phi_{ext}^{12}}\right|$$

$${GCI_{fine}}^{21} = \frac{1.25\ {e_a}^{21}}{{r_{21}}^p - 1}$$

What is written for 21 (Medium - Fine) relationship is intended for 32 (Coarse - Medium) as well. Hence, if the mesh geometry is well thought and realized, or in other words providing for a blocking strategy that doesn t bring to regions of high warped or skewed elements, the values should converge to the target one as the mesh becomes finer. The number of elements, and so the mesh grain, is chosen on the bases of the data convergence within a tolerance stripe of 2%. But as we could see further, some employed meshes are finer than the ones selected with this method; those are the ones used for Transient simulations, and the only reason is to have more broad boundaries on the Courant analysis-based timestep selection.

	MESH	N	h	r
3	Coarse	210858	3.50492	
2	Medium	673483	2.37994	1.47269
1	Fine	1855376	1.69771	1.40185

Table 3.1: Course, Medium and Fine Mesh Data

Richardson analisys would require as reference values general parameters but, since there aren t real *General* Values in our experiment, we examine Local parameters such Pressure and Velocities at several Points. The ratio on which the mesh choice will be based will thus be the convergence of several parameters, depicted in a normalized value (based on the target one) along the normalized mesh size. The values taken in account to check the mesh convergence have been randomly picked: those are velocity and pressure in Pgap, Vel I53.

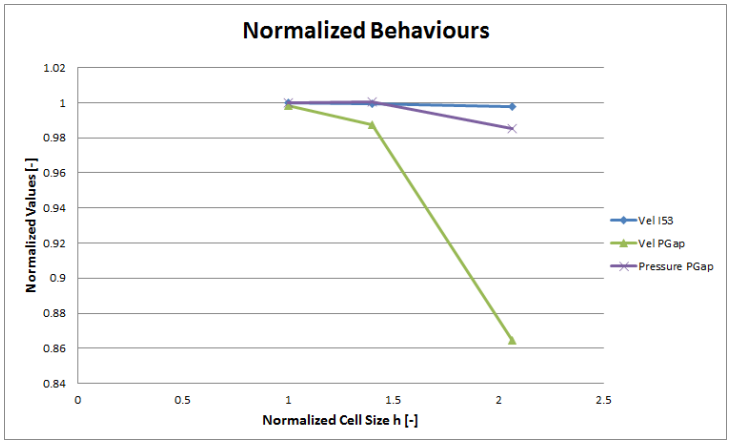

Figure 3.2: Behaviours of the chosen Values

	Velocity		Pressure
	I53	Pgap	Pgap
Phi1	28.660	31.888	198.245
Phi2	28.649	31.533	198.353
Phi21ext	28.664	31.940	198.239
GCI21fine	1.88E-04	2.02E-03	3.84E-05
GCI32medium	6.50E-04	1.61E-02	6.93E-04

Table 3.2: Table showing the analisys outcomes, including the GCI and the reference value (the green stripe)

Since we have preaviusly decided a 2% error, the Medium Mesh is chosen for the steady state simulation, and only to highten the bound of the timestep extent according to the Courant condition, the Fine mesh is taken for the Transient simulations.

3.4 The Selected Meshes

Here are provided some geometrical infos of the Medium mesh.
Measures of mesh orthogonality, expansion and wall ratio are usually referred as quality parameters of the mesh. The mesh resolution is defined by y^+. Here are data:

Minimum distance: *All the distances in millimeters*

- On the side walls: /Total Distance:10.1376/ Nodes: 20 / Min.Space: 0.0115484 / Ratio: 1.3
- On the Airfoil: / Total Distance: 9.88073/ Nodes:20 / Min. Space: 0.0162461 / Ratio: 1.3

- Up and down: / Total Distance: 50 / Nodes:40 / Min. Space: 0.05 / Ratio: 2 (On both directions)
- On the Gap: / Total Distance: Variable / Nodes: 10 to 15 / Min. Space: 0.016 / Ratio: 1.6 (On both directions)

For the most sensitive near-wall regions in order to determine the depth of the first cell y^+ PointWise calculator has been employed, taken from `http://www.pointwise.com/yplus`. For the value to be calculated, the undisturbed velocity and density has to be supposed. However, y^+ in all the simulation is resulted below 5.

We give in conclusion some depictions of the chosen Medium and Fine mesh, to convey a general impression on the meshes will undergo the CFX Simulation.

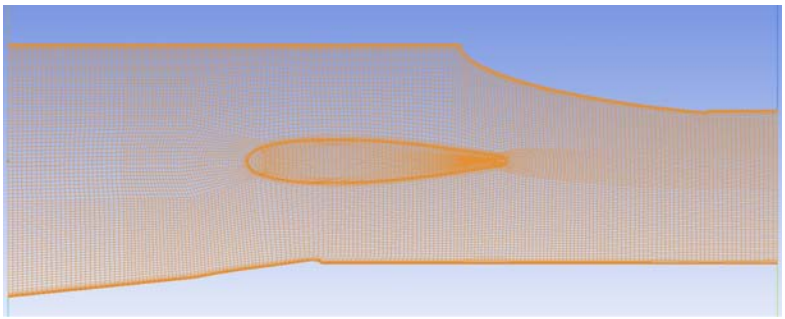

(a) Medium Mesh

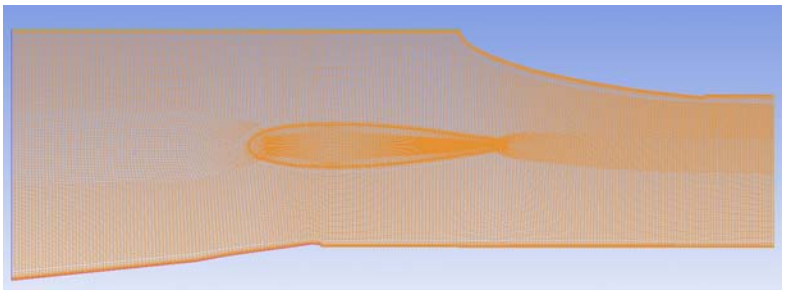

(b) Fine Mesh

Figure 3.3: Depiction of the selected meshes

Chapter 4

Simulations

All the calculations are performed with three-dimensional Navier-Stokes solver ANSYS CFX 13.0 Software. This tool is preferred to Fluent for more experience of the user and more ductility in the use.
Thus, it is decided to set the simulation in CFX-Pre, to exploit the integrated tools downstream (among whom there is CFD-Post) better. After setting the general folder in CFX-Pre the mesh is imported setting millimeters as basic units. Then the boundary conditions are set, sorting the groups of surfaces by the mesh parts prearranged in ICEM CFD. The boundary conditions are set in order to allow an handy downward setting of the simulation. So they are separated in *Airfoil*, corresponding to the movable central profile, *Inlet* and *Outlet*, obviously kept separated, and *Wall*, that encloses all the other surfaces that mark the domain. Before getting into the simulations some clarifications are needful: first of all, the fluid employed in the simulation is Air at 25 C, already present in the Fluid Library of the program, aiming to follow the Paper [1] prescriptions, while the temperature is just supposed. Eventually, the sections of measurement corresponding to Inlet, upstream from the profile, and Section 1, downstream, useful for the further analysis, are here displayed:

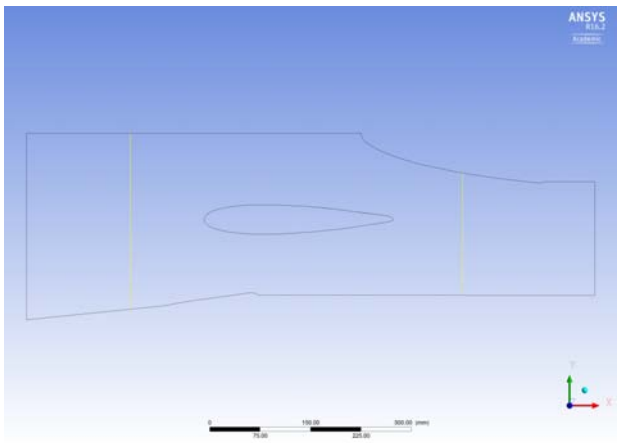

Figure 4.1: Position of the Measurement Sections taken in account

4.1 Steady State Simulations

The steady state simulations are the easiest ones: easy to monitor in Solver Manager Tab their convergence depends upon the employed turbulence model and can easily be reached and detected when RMS residuals of the balance equations approach to zero. Since the Steady State model is an approximation of the real phenomena, this tool should be employed only in predictable quasi Steady situations. In our model, high closing angles lead surely to the rising of unsteady flow structures located in the rear of the profile, so those simulations are only performed in transient state, or rather an initial SS simulation is made only to work as initial values set for the transient one. Hence, only the cases with no closing angle are performed. The simulated Cases are:

- Gap 0 mm; 0 Degrees
- Gap 0.2 mm; 0 Degrees
- Gap 0.4 mm; 0 Degrees
- Gap 0.6 mm; 0 Degrees
- Gap 0.8 mm; 0 Degrees
- Gap 1 mm; 0 Degrees
- Gap 1.5 mm; 0 Degrees

Or rater, all the Gap considered by the original paper [1]. Through these sets of simulations, several data are collected, to validate and make further studies on theoretical approaches disclosed by the underlying literature on the leakage flow issue. In detail, as it will be treated on the following chapter, critical reviews on the flow rate and the trend of average pressure difference between pressure and suction sides. Then, several monitoring points are arranged in order to check the system convergence. Those points are all the points from measurement Section 1, plus a point set in the middle of the chord span, between the gap and the covering plate, which is supposed to be the most sensitive part for convergence criteria.
The settings are the following:

- Analysis Type: Steady State
- Default Domain Settings: Domain Type: Fluid Domain
- Fluid Employed: Air at 25C, present in Fluid library
- Morphology: Continuous Fluid
- Reference Pressure: 1 atm
- No Mesh Deformation

Boundary Conditions:

- Airfoil: Wall, no slip wall, smooth wall
- Inlet:
  - Flow Regime: Subsonic
  - Mass and momentum: Normal Speed, 25.446 m/s
  - Turbulence: High Intensity (10
- Outlet:
  - Flow Regime: Subsonic
  - Mass and Momentum: Average Static Pressure, 0 MPa, Pres. Profile Blend 0.05
  - Pressure Averaging: Average over whole Outlet

- Wall: Wall, no slip wall, smooth wall
- Solver Control:
  - Advection Scheme: High Resolution
  - Turbulence numerics: First Order
  - Convergence Control: Min. Coeff. Loops: 1; Max. Coeff. Loops: 500
  - Timescale Control: Auto Timescale
  - Length Scale Option: Conservative
  - Convergence Criteria: Residual Type: RMS Residual Target: 1e-06 s
- Output Control: Monitor Points: All Gathering points of measure section 1, plus a point close to the rear of the GV in the high pressure wake, another one in the Inlet section, and the last one in the Gap span, approximately in the centre of the profile.

The convergence history is quite standard and short, meaning that the Mesh is robust and well built. Naturally, as the Gap increases turbulent phenomena tend to gain relevance, leading to a more unstable convergence behaviour. We display here 0.6 mm Gap case for reference, compared with the case of maximum Gap simulated.

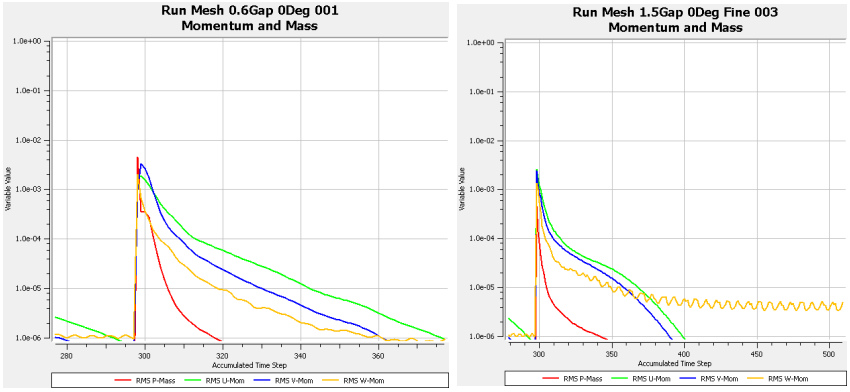

(a) Gap 0.6 mm 0 Deg RMS (b) Gap 1.5 mm 0 Deg RMS

Figure 4.2: Convergence history of Steady State simulations

4.2 Transient Simulations

The simulations are set to survey the leakage vortex better, highlighting flow transient structures and the unsteady phenomena at the rear of the airblade. Appropriate Monitoring Points are set to detect the pressure and velocity pulsation and to determine when the simulation has converged. based on the structure of the diagram Velocity-Simulation time. Firstly the SST turbulence model is applied, and then for a better understanding it has been chosen to apply the SAS SST Turbulence model. Infact, since with SST model no difference is spotted with the Steady State simulation, SAS model is preferred, and for obvious reasons only with SAS model transition processes are here described.

4.2.1 Courant Analysis

In order to settle the timestep duration properly, the Courant number theory has been applied. The Courant Number expresses the ratio between the distance treaded by the flow in the selected

Timestep and the Mesh size. In 3D environment, it is defined as follows:

$$\nu = \frac{u\ \Delta t}{\Delta x} + \frac{v\ \Delta t}{\Delta y} + \frac{w\ \Delta t}{\Delta z}$$

Where u is the axial component of the velocity, Δt is the selected timestep and $\Delta x, y, z$ the dimensions of the cell. In order to bring a simulation to convergence, the time step must be less than the time employed by the flow in any point to move from one cell to another. This is known as the Courant Condition [3] , that essentially expresses $\nu \leq \nu_{MAX} = 1$ bound . Given the Number definition, such condition expresses itself giving an upper bond, indeed, for the value of the timestep, that will be calculated with the:

$$\Delta t \leq \frac{1}{\frac{u}{\Delta x} + \frac{v}{\Delta y} + \frac{w}{\Delta z}}$$

As velocities we will chose $u = 40\ m/s$,$v = 5\ m/s$ while z component is neglegible, as cell dimensions we will set $\Delta x = \Delta y = \Delta z = 1.25\ mm$, charateristic of the finer mesh, that is indeed used for the Transient simulation , in order to move the courant condition to higher values. The resultant value is $\Delta t = 2.77\ 10^{-5}\ s$. Nevertheless this value is too computationally heavy, so trusting in ANSYS ability to keep convergence, $\Delta t = \ 10^{-4}\ s$ is set as timestep.

4.2.2 The Simulations

Most of the cases disclosed by [1] deserve to be simulated, but since the simulations takes several days to being completed, we will focus only on some relevant cases. Among the most important ones lays surely the cases of the maximum Gap span, since it is predicted that the arising of a vortex flow will have its maximum intensity and unsteadiness, so all the cases investigated, except for one, will be with 1.5 mm of Gap. The tests are:

- 1.5 mm Gap 0 Deg,
- 1.5 mm Gap 10 Deg
- 1.5 mm, rotation until 4 Deg is reached

Two different `.ccl` files are set in order to cover the requirement of all the simulations. The first aims only to investigate a static geometry, and is indeed used on the three non-variable geometry cases. Its parameters are:

- Analysis Type: Transient
  - Total Time: 5 s
  - Timestep Duration: $10^{-4}s$
  - Initial Time: 0 s
- Default Domain Settings: Domain Type: Fluid Domain
- Fluid Employed: Air at 25C, present in Fluid library
- Morphology: Continuous Fluid
- Reference Pressure: 1 atm

- No Mesh Deformation

  Boundary Conditions:

- Airfoil: Wall, no slip wall, smooth wall
- Inlet:
  - Flow Regime: Subsonic
  - Mass and momentum: Normal Speed, 25.446 m/s
  - Turbulence: High Intensity (10
- Outlet:
  - Flow Regime: Subsonic
  - Mass and Momentum: Average Static Pressure, 0 MPa, Pres. Profile Blend 0.05
  - Pressure Averaging: Average over whole Outlet
- Wall: Wall, no slip wall, smooth wall
- Solver Control:
  - Advection Scheme: High Resolution
  - Transiens Scheme: Second order backward Euler
  - Timestep Sizing: Automatic
  - Turbulence numerics: First Order
  - Convergence Control: Min. Coeff. Loops: 1; Max. Coeff. Loops: 10
  - Timescale Control: Auto Timescale
  - Length Scale Option: Conservative
  - Convergence Criteria: Residual Type: RMS Residual Target: 1e-06 s
- Output Control: Monitor Points: All Gathering points of measure section 1, plus a point close to the rear of the GV in the high pressure wake, another one in the Inlet section, and the last one in the Gap span, approximately in the centre of the profile.

The other `.ccl` file is expressly realized to simulate the closing movement of the central Guide Vane. The rotation movement of the airfoil is realized by the Cartesian rotation expressions implemented in the Expression section, and then assigned to the airfoil surface in the boundary conditions. The equations are modified to adapt CFX-pre language, or rater let the deformation of the original mesh to follow the rotation of the surface.
The main reason of this test is the determination of the approximative value of the closing angle at which turbulence strengthening at the rear suction side becomes relevant, and aside from this also to determine and display the changing in position and structure of the leakage vortex. The differences between the previous `.ccl` file description are only in the Expressions set to rotate the profile:

- Definition of rotation center $(X_0, Y_0, Z_0) = (395.41, 0, 0)\ mm$
- $AngVel = -10\ degree/s$ Angular velocity of closing

$$NewX = ((x - X_0) - TotalMeshDisplacement\ X)\ cos(AngVel\ t) + ((y - Y_0) - TotalMeshDisplacement\ Y)\ sin(AngVel\ t) + X_0$$
$$NewY = -((x - X_0) - TotalMeshDisplacement\ X)\ sin(AngVel\ t) + ((y - Y_0) - TotalMeshDisplacement\ Y)\ cos(AngVel\ t) + Y_0$$
$$NewZ = ((z - Z_0) - TotalMeshDisplacement\ Z) + Z_0$$

The rotation is possible only for some degrees (around 4), after which the mesh become too deformed and convercence problem arise.

Finally, two convergence histories for transient simulations are presented, where the influence of turbulence on the RMS residuals can be spotted.

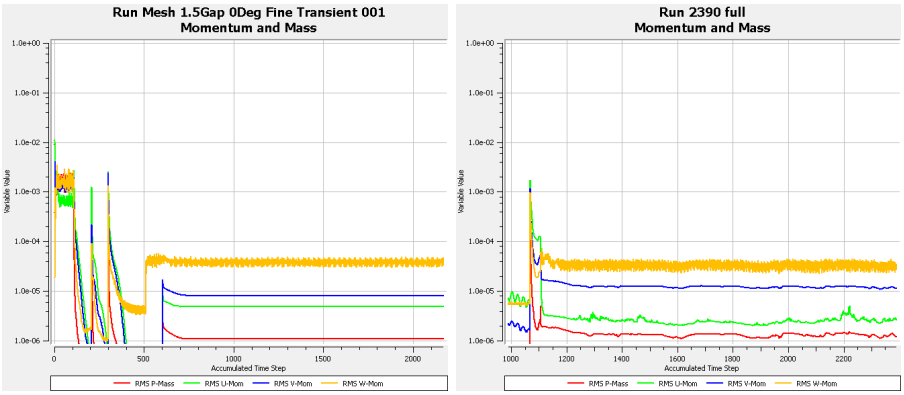

(a) 1.5 mm Gap 0 Deg (b) 1.5 mm Gap 10 Deg

Figure 4.3: Convergence history of Transient simulations, it can be seen the influence of turbulence on the Residuals

Chapter 5

Results

In this chapter the results for all the driven simulations are presented. The data gathered from CFX simulations are compared to the experimental ones, providing a judgement on the reliability of the simulated data. Then, the steady state simulations are introduced; through several graphics and pictures, a general idea of the flow structure behaviour is pointed out, aiming to highlight the shape and dimensions of leakage vortex and to make a comparison between the flow field with and without leakage Gap. The transient simulations are then introduced along with a brief comparison with the SS results. Finally, a general examination on the leakage flow rate is carried out.

5.1 Steady State - Experimental Data Comparison

This multiple section of comparisons will be carried out exploiting excel flexibility in big data handling. The experimental data, only available on paper support, are manually inserted on the Excel file. When the simulations are performed the grid of monitoring point is loaded by the `AcquisitoreDati.cst` file. Enclosed with the file, a table including values of pressures, x and y velocity components at 1 and Inlet Sections is loaded, obtained in the same monitor points used in the experimental test. The table is then loaded in the same excel file, which has been preaviously divided in three sections:

- Calculations: Where are made the comparison plots
- Comparisons: Where is made the statistical distribution plot
- Data: Where all the data are stored

The first comparison plots is now presented:

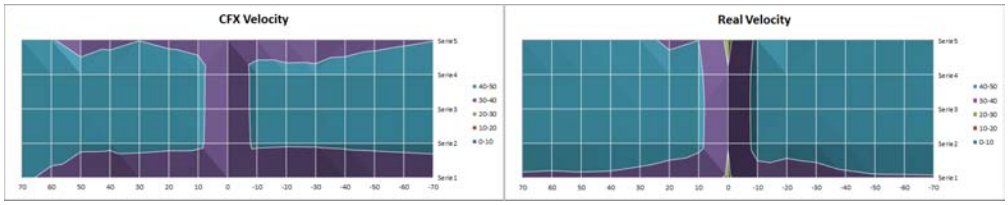

(a) Gap 0 mm

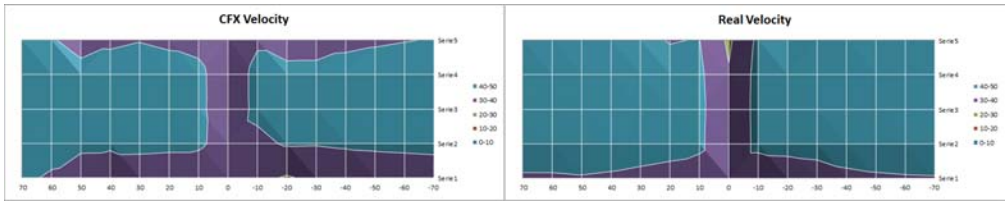

(b) Gap 0.2 mm

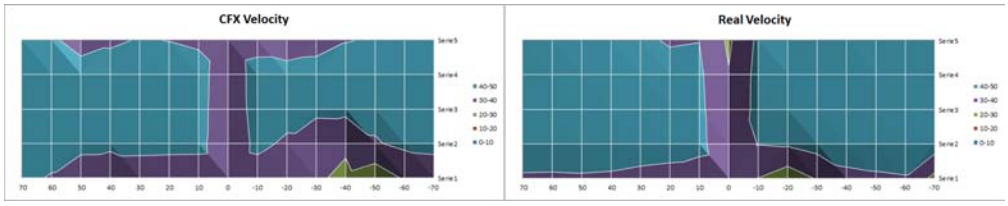

(c) Gap 1 mm

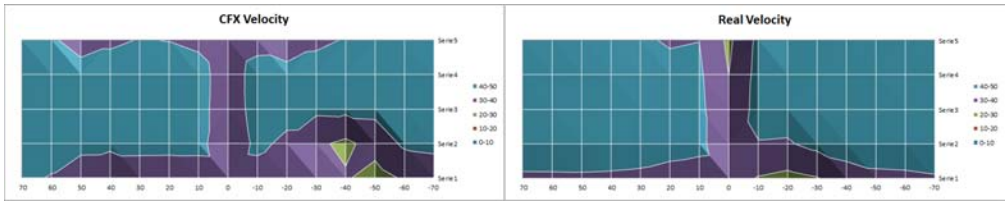

(d) Gap 1.5 mm

Figure 5.1: Comparison between calculated and Experimental values of the velocity pojection on x-y plane at measurament Section 1 in the specified Cases

The two compared velocity fields appear with the same general outlook. It is, for instance, in both clearly visible the lower velocity region belonging to the central profile wake. Nevertheless, the difference between the two fields is quite substantial and systematic. First of all the velocity drop near the walls, besides the inferior part, doesn't clearly show up in the experimental values like in the computational ones. Consistely, the real downstream wake of the central profile seems to be slower than the simulation would remark. The computational data also point out the existence of the horseshoe vortices, arising from the interaction of the flow with any kind of obstacle embedded between two walls. Those vortices originate near corners and junctions and then move forward and propagate downstream. While around the central profile are overtaken by the wake and the local turbulence, those structures are clearly noticeable along the left GV span, and are captured in the velocity profile of Section 1.

When the Gap increases, in the simulated data the leakage vortex presence is clearly high-

lighted, at first as a region of low speed joined within the profile wake, and then as a single entity that begin to occupy a region of plan further from it. Nonetheless, this trend is not highlighted in the experimental Data; even though they show a low speed region on the right side of the wake, they don t display it neither as pronounced nor as detached from the profile wake. Hence, the most evident conclusion is that in the experimental velocity field all the swirling structures (both leak and horseshoe vortices) occupy less space in the main flow. This tendency seems to be confirmed also by document [25], in the velocity profile plots. Some hypothesis can be made to explain this tendency.
Looking at the leakage vortex, the simulation appear to have overestimated the flow rate through the Gap, that, directly linked to the Gap velocity profile, might have lead to a consequent increase of the downstream eddy structure. Another and general hypothesis might be the overall underestimation in the simulations of the blending power carried out by the turbulence inside the velocity field. This seem to be strengthened considering that the specific deviation between the two average velocities on section 1 (directly bounded to the flow rate across the considered surface) is small, not exceeding 5%.

Gap [mm]	Dev. Ave. Vel. [%]
0	4.53%
0.2	4.82%
1	4.14%
1.5	4.04%

Table 5.1: Percentual differences average velocity on Section 1

However, conversely from the punctual values, the general parameters appear to be closer to the experimental ones, so the cause of the local discrepancies must be found in the local mechanism of momentum diffusion, while the overall results remain reliable. This tendency is also confirmed by the inlet section, whom experimental velocity profile, without a sensitive difference in the mean value, shows a much more even local average velocity, although more turbulent, than its simulated equivalent.
We can identify different two possible causes of this difference in turbulence blending:

- An input mistake: At the inlet section, the real model could have had an higher turbulence, gained along the upstream path (the flow has to cross a blower and a convergent air duct), that couldn t have been predicted by the software since the turbulence value had already been set up at the maximum value.
- A wrong turbulence model selection: as already shown, it has been employed the SST turbulence model. That proved to be the best in terms of convergence stability and trust of the generated data. Moreover, among the turbulence models checked ($k-\omega$ and $k-\epsilon$) the SST model has exhibited the smallest turbulence structures. For these reason, although not tightening to reality, this model remains the best choice.

Another additional element of uncertainty could have been correlated to the Anemometer, whose neither uncertainty nor the size of the scale are known. Finally, the plots referring to the correlation Coefficient calcolated for the punctual values are presented. As it can be seen a turbulence enhancement (trough Gap increase) leads to a fewer local values matching.

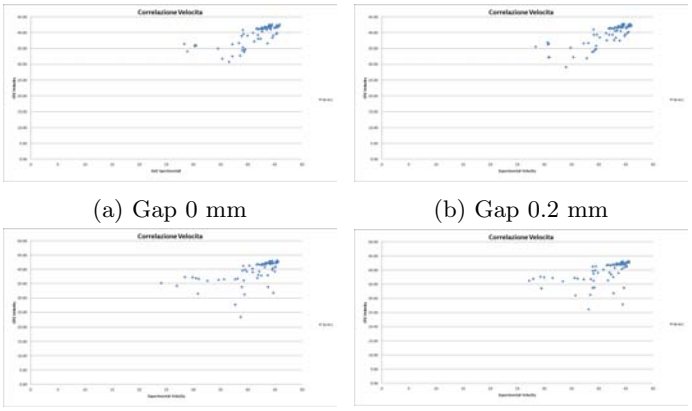

(a) Gap 0 mm (b) Gap 0.2 mm

(c) Gap 1 mm Nose (d) Gap 1.5 mm Rear

Figure 5.2: Correlation Coefficient Plots

Gap [mm]	Corr. Coeff.
0	0.750955004
0.2	0.79875478
1	0.579982643
1.5	0.536261606

Table 5.2: Table showing the correlation coefficient along the Gap

5.1.1 Integral Parameter Study

As we will discuss later in this document, the model, given its structure, doesn t allow the formalization of any reliable recapitulatory parameter useful for both the present analysis and the possible real situation. Some important parameters might have been formalized: a swirl number, defined in a way similar to the second multi stage pump inlets, namely calculated like the ratio between the integral of the overall velocity field and the integral of the main velocity component (or rather the velocity component of interest). Determined in this way, the parameter becomes a sort of efficiency measurement that compares the importance of the main flow related to the disturbances. In this situation, the reference section on which this parameter is calculated, is not in the same direction towards which the real flow is supposed to be turned, hence owning some distortion in the parallel velocity component that can be neither neglected nor removed.
Being aware of that, it will be tried to formalize an integral parameter, having no intention to provide an efficiency measure, but rather in order to make a conclusive and consistent comparison between CFX and Exp Data. The importance of this parameter may establish the global level of the simulation, and through its discrepancy between Experimental and CFX will be indeed provided an overall check of the quality of the work made. So this swirling number is defined as:

$$FP = \frac{\int_A v \, dA}{\int_A \vec{v} \cdot d\vec{A}}$$

As it has been said this parameter alone is not explicative of the entity of the disturbances, since in the Section 1 the axial velocity ($\vec{u}$ component) is not the only reference velocity in all the section because the streamline paths, following the shape of the left Guide Vane, execute a correct bent trajectory.

The evaluation of the two Flow Parameters yields:

	Flow Parameter
Experimental	1.010377244
CFX	1.007415034

Table 5.3: Comparison of flow parameter between Transient Computational and Experimental Data

Hence, the percentual specific difference is:

$$Sp.\ Difference = 0,29\ \%$$

Almost neglegible for the pourposes of this study.

5.1.2 Reliability Considerations

It has been widely demonstrated how the punctual values do not perfectly match to each other, while the overall parameters, excepting from a natural negligible percentage of error, appear to be closer to the experimental situation. This latter tendency is confirmed by the average velocities of the inlet section, aside from the already shown velocities in Section 1 and the flow parameters. Luckily, our study does not concern any local value, as we will work only with integral and averaged parameters (ave velocity, mass flow rate, Flow Parameter). We are therefore considerably sure about the validity, under a certain percentage of error, of all the studies that will be later disclosed included in the SS section.

5.2 Steady State Data presentation

The first and most obvious way to have a panning shot on the results and the most suitable format for them to be displayed is surely trough velocity plots at Inlet and First measurement section:

Aside from those pictures, it has been noticed that there is asymmetry between superior and inferior parts also in the cases with no Gap, this is probably because we are surveying in steady state an up and down pulsating phenomenon, so the transient simulation would be useful even with the most time-independent simulation.

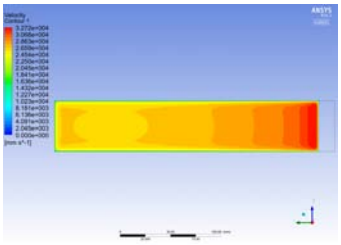

(a) Inlet Section

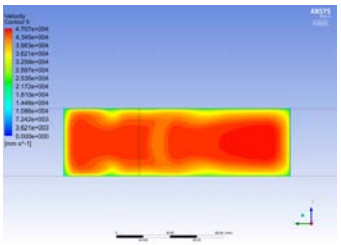

(b) Section 1; 0 mm Gap

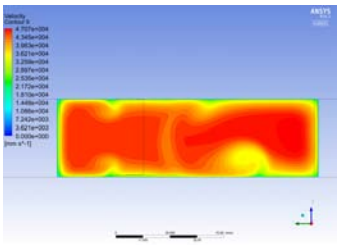

(c) Section 1; 1.5 mm Gap

Figure 5.3: A first glnce of the flow field

Then, since one of the main aim of this work is to highlight the nature of the flow structure, the development of the leakage vortex, that is one of the most important flow characteristic, is shown. The following picture encloses streamline plots taken at the nose and rear section of the profile for all the considered gaps.

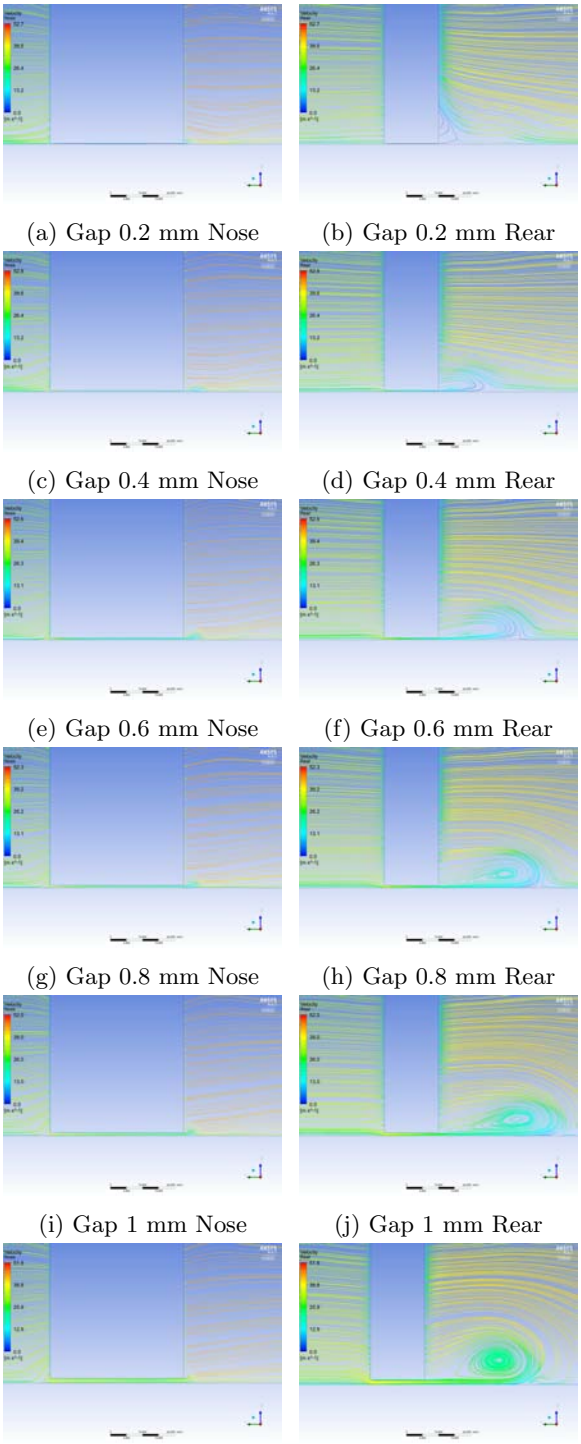

(a) Gap 0.2 mm Nose (b) Gap 0.2 mm Rear

(c) Gap 0.4 mm Nose (d) Gap 0.4 mm Rear

(e) Gap 0.6 mm Nose (f) Gap 0.6 mm Rear

(g) Gap 0.8 mm Nose (h) Gap 0.8 mm Rear

(i) Gap 1 mm Nose (j) Gap 1 mm Rear

(k) Gap 1.5 mm Nose (l) Gap 1.5 mm Rear

Figure 5.4: 2D Streamline Plot around the bottom side of the GV, back and forward section

2D streamline plots: The pictures show clearly how the leakage vortex is always located on the suction side and how its development starts regardless from the gap span beyond the half span of the profile. Along the profile span the flow coming out from the Gap, at high tangential component, meeting the main flow creates the vortex. Moreover as the Gap increases:

- The vortex relevance increases, even though it presents an asymptotical approach.
- The vortex detaches from the profile, whom for small gaps was close to.
- The vortex arises at progressively smaller chord span, closer to the leading edge.
- Internal velocity tend to increase, but this growth is progressively softened as shown in figure 5.6b

The front part instead, never shows the vortex presence: the streamlines follow a straight path. Later, a series of pictures depicting a cromathic plot of the Turbulence Eddy Dissipation on the Plane 1 is shown:

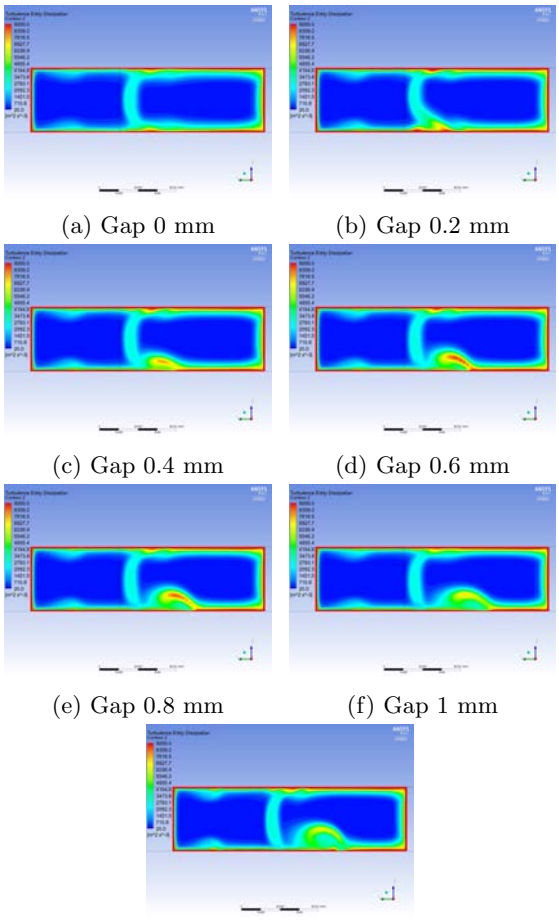

(a) Gap 0 mm (b) Gap 0.2 mm

(c) Gap 0.4 mm (d) Gap 0.6 mm

(e) Gap 0.8 mm (f) Gap 1 mm

(g) Gap 1.5 mm

Figure 5.5: Turbulence Eddy Dissipation Plot comparison at Gap increase

Turbulence Eddy Dissipation: Those graphics are shown as additional term of comparison and also as partial marker of the additional inefficiency source brought by the vortex presence. When the Gap increase:

1. The dissipation structure, tightly bounded to the vortex structure
2. Nonetheless, the strength of that dissipation diminish, and this leads to a Turbulence Eddy Dissipation rate roughly constant, or rather slightly growing

Moreover, in the pictures are also pointed out the dissipative structures associated to the horse-shoe vortices and those generated from the interaction with the walls.

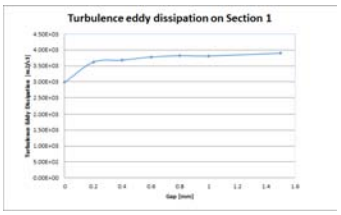

(a) Trend of Turbolence Dissipation Rate along the Gap

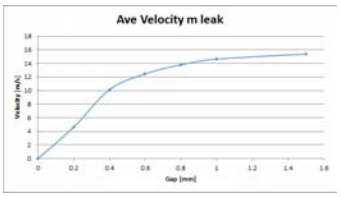

(b) Trend of average velocity through the Gap as it increases

Figure 5.6: Different values plotted against Gap

One of the two important studies that this thesis aims to perform, along with a better clarification of the leakage vortex entering the runner, is a rough quantification of the total energy loss due to vortex presence. This, since the working fluid is supposed incompressible, without leaks trough the model is deeply bounded to the overall pressure loss between Inlet and Outlet section, here displayed:

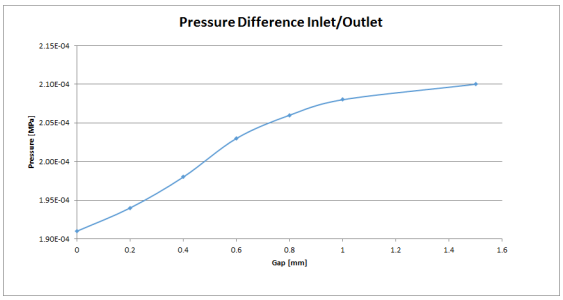

Figure 5.7: Trend of the pressure difference between Inlet and Outlet Sections

The Gap influence is at the beginning very strong but it tends to soften for higher Gap span, showing a slight asymptotical approach.

5.3 Transient Simulations Data

All the data presented in this section have been obtained by using the SST SAS Turbulence model, currently one of the most accurate avaliable on CFX. Given the relevant amount of cases

likely to be simulated, it has been decided to optimize the process running only those that have the maximum Gap span, where leakage vortex and turbulent structures are most likely to be found.
The specific task of this transient investigation is the visualization of the turbulence displacement along the model. The mean employed in order to provide a quantitative marker of this fluctuations is here Velocity plots against Accumulated Timestep, taken is some relevant places. Moreover, these Data sets are used beacuse they allow several other considerations, such as the determination of the turbulence ratio for specific points and the chance to understand if after a certain number of settlement iteration an overall periodic behaviour can be spotted.

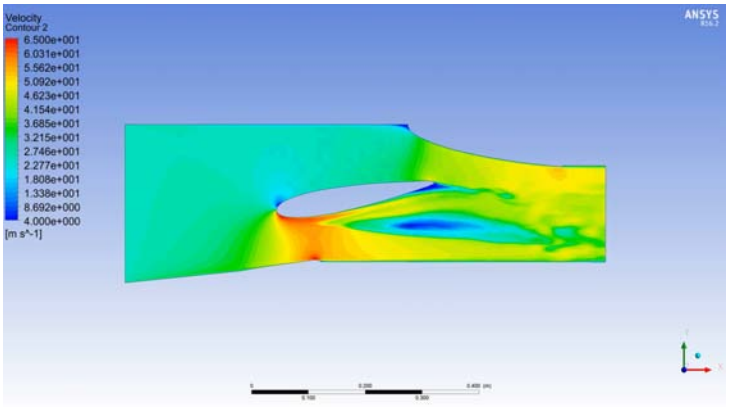

Figure 5.8: Shot of the Transient simulation Results 1.5 mm and 10 Degrees; the two main turbolent structures, leakage vortex and profile wake, can be easily spotted by their Kolmogorov vorticies

All the graphics plot velocity. In order to take in account the turbulence intensity the Reynolds Decomposition has been employed:

$$u(x,t) = U(x,t) + u'(x,t)$$

$$u_{rms} = \sqrt{\langle u'^2 \rangle}$$

Where the ratio u_{rms}/U stands for the turbulence intensity. With reference to the low angle the 0 Degree case will be discussed, by showing the velocities of two points: the first called *Rear* is located at middle height right behind the profile, in one of the most intensive turbolent zones, it provides the maximum turbulence intensity among all the model. The second one, called *P103*, is one of the measurement points of the experimental test rig, located further within the profile wake at medium height span, a point downstream from the turbulent source.

The values are in m/s, while 500 Timesteps are included, corresponding to $0.05s$. The plots might be affected by some uncertainty or some failure within the calculation, but the values among which the velocity fluctuates are considered reliable. The turbulence intensities are hereby calculated:

$$TurbulenceIntensity$$

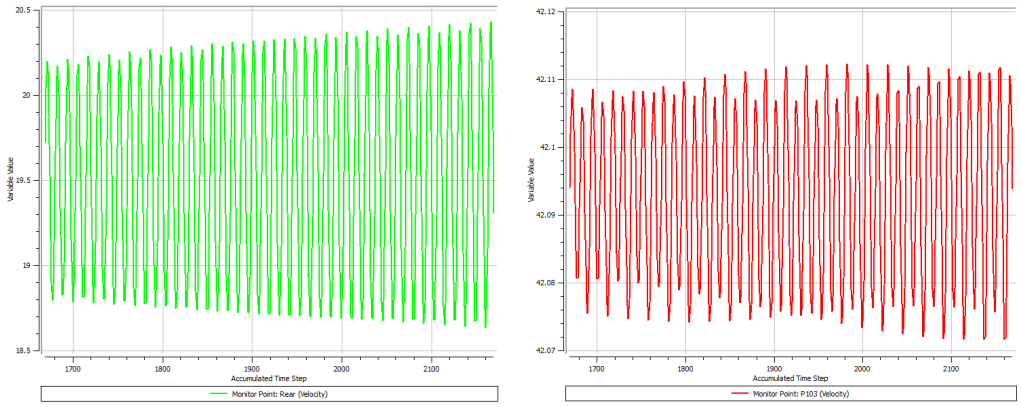

(a) Rear Point (b) P103 Point

Figure 5.9: Velocity VS Accumulated Timestep Graphics for maximum Gap and 0 Degrees condition, 500 Timesteps

$$Rear : 4.6\% \quad P103 : 0.047\%$$

In the same points the situation at high closing angles is highly different:

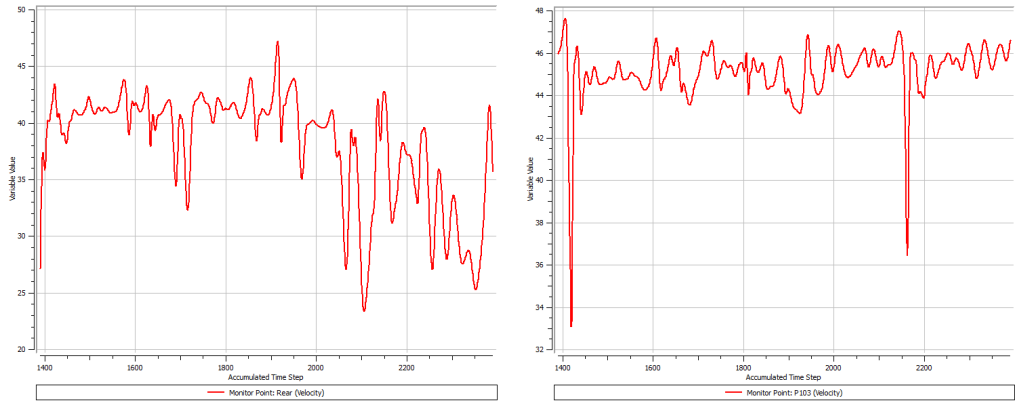

(a) Rear Point (b) P103 Point

Figure 5.10: Velocity VS Accumulated Timestep Graphics for maximum Gap and 10 Degrees condition, 1000 Timesteps

At 10 degrees the turbulence is too intense, a slight periodic behaviour can be characterized only in P103; Transient simulations are therefore important for those cases. The last simulation is a test of closing rotation at 10 deg/s, in order to see at which angle the turbulence arises.

It turns out that this phenomenon arises at nearly 1900 Iterations, namely nearly 4 Degrees. In conclusion, the general trend is that the turbulence increases with the closing angle and not with the Gap span.

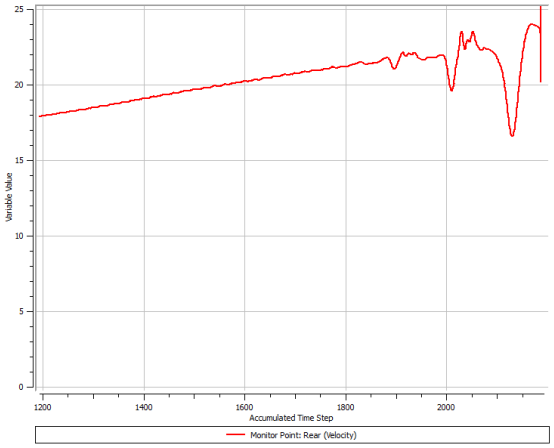

Figure 5.11: Velocity plot at Rear point

5.3.1 SS - Transient Data Comparison

The Transient results, in relationship with the SS ones, can show three different outcomes:

1. Being nearly steady, showing a very low propension to time variations.

2. The Vel/Pressure field can present remarkable periodical fluctuation patterns.

3. The turbulence can lead to chaotical and unpredictable values variations.

The first case, provided that the fluctuation is really low, wouldn' t require a transient simulation and could be fully described by an SS one. In the second case, since in order to have a periodic trend the fluctuations are not supposed to be too drastic, the Steady State simulation may portray a time-averaged like situation, still being tight to reality and having a descriptive meaning. In the third case as it can be easily understood, the strady state simulation loses all its descriptive value remaining a mere tool for a general visual understanding.

The high angle cases fall into the third condition, so no comparisons can be seariously performed. The low angle cases instead, are similar to the first condition so it is proceeded to an SS and time averaged Transient Data comparison in order to verify the general modulus matching. Here is compared the average value of velocity on Section 1 as example:

$$Sp.\ Difference = \ 0,61\%$$

Therefore, the percentual difference is neglegible. In conclusion, since the turbulence intensity is low as above demonstrated, the resemblance between SS and Transient simulation that this latter step for low angles can be completely skipped. Whichever the value of Gap span, the Steady State simulations totally fullfill all the requirements.

5.4 Leakage Flow Rate

From licterature [5, 9] it has been found an empirical formulation, derived from Bernoulli continuity equation, predicting the leakage flow through a clearance Gap between two stationary Walls.

$$Q_l = A\mu\sqrt{2g\Delta h}$$

Where Q_l is expressed in m^3/s, A stands for the area of the Gap section, g is the gravitational acceleration, Δh the pressure difference betwen the sides expressed in m, and finally μ is the flow coefficient, determined by experimental data as:

$$\frac{1}{\mu^2} = 0.0011\left(\frac{l}{s}\right) + 1.6097$$

Simultaneously, defining a surface that covers all the Gap span, the values of Leakage Mass Flow Rate have been collected for every Gap. The plot comparison between those Data yields:

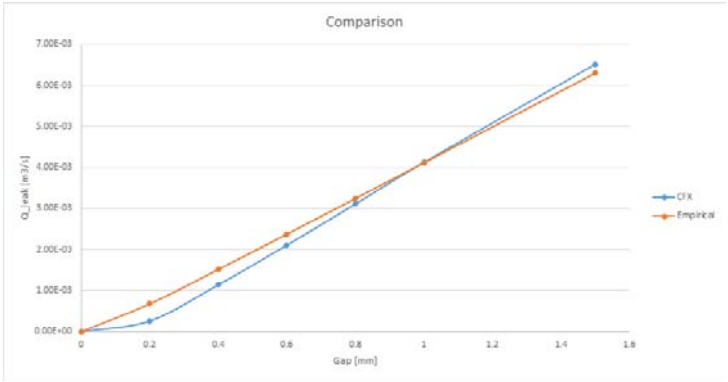

Figure 5.12: Leakage Flor Rate Comparisons

The formula calculates an almost perfect linear tendency and the simulated data seem to agree, except for a little flow overestimation at small Gaps.

Discrepancies between simulated and empirical flow rate: This formula has been built considering [9] pressure diference and constant Gap width. However, this is not the real situation happening in the profile gap, for several reasons:

- The pressure difference is not constant along the profile progression
- The path of the leakage flow is not constant too, it depends upon the profile region and the angle of the flow at the gap entrance.
- Even though the experimental Data don't take in account that, in the real situation the Gap span is not constant, but, since it is caused by erosion, strongly rough and uneven.

Nevertheless, the resemblance is quite satisfactory, and we can say that the formula has been further verified with this study.

Chapter 6

Further Work

This final chapter gives some suggestions and hints to be used if it is decided to proceed and develop further studies on the matter, which is strongly to be hoped. Within an idea of deep investigation towards the detailed quantification of the phenomenon, this model is worth to be considered an initial step, useful to highlight the most relevant features involved (like the leakage flow and the vortex whom it generates downstream) and to gather the necessary preliminar information for the construction of another more detailed one, that will become the main source of data. In this chapter then, it will be both briefly discuss the flaws of the present model and give some suggestion for the new one.

6.1 Effective validity of the model

The model is not intended to represent the real situation, it is indeed only meant to work as data gatherer for the preliminary phase of the studies. So it is essentially unable to reply the reality for several reasons, which will be discussed below. The first reason is the equipment of a flat inlet: its shape, indeed flat and arranged perpendicularly to the central profile, has a remarkable affection on the stream paths, preventing it from having a curved structure, which would have been similar to the one experienced in the real operational condition of that GV portion. Infact, while in the real GV section the flow follows the free vortex law, marked by $r\ c_u = cost$, in the model the entrance is straight ahead, so the flow enters with a constant angle equal to the GV initial inclination and if it wasn t disturbed it would proceed following a straight path instead of a curved one, predicted by the above quoted law. Nevertheless, in its path the flow encounters the profile and deals with the channel shape that modifies its overall orientation towards a curved realistic path; but however the outlet shape, flat and parallel to the inlet, plus the presence of the left wall eventually prevent the development of conditions closer to reality. This characteristics affects the outcome of the experiment forcing the data output to undergo a critical interpretation and a further adjustment to be considered approximately representative of the real situation.

Height of the model: the model height is only 50 mm, smaller than from the real inlet span, so, even though the span is sufficient to bring the vortex structure and all the related side effects to a completed development, the flow structure can t be completely portrayed. The lost info regard especially the effects in the pulsating velocity and pressure field due to the interaction between the upper and the lower vortex with each other as well as with the main flow.

Flat measurement sections: The measurement sections are therefore coherent with the

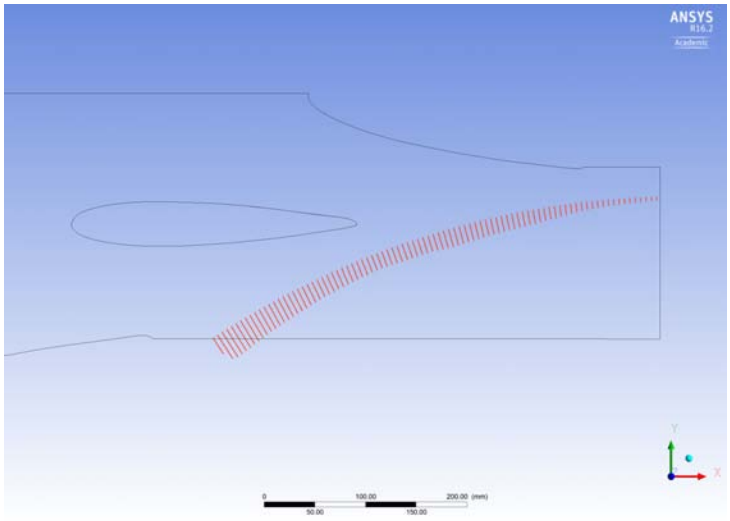

Figure 6.1: Decreasing distribution of the normal component of the velocity, main flaw of the model

Outlet/Inlet sections, so they are distributed in a region different from the runner inlet. Hence, it is impossible to lead the acquired data back to the latter distribution. This disable every possibility to acquire from the so-gotten data some sort of parameters that have some validation in a more realistic situation. Another issue are the fixed side Guide Vanes and Walls: the two side guide vanes are embedded in the model and can t change either angle or Gap to follow the central one movements. This is perhaps the most relevant problem, creating an unacceptable side effect that affect all the experiment.

Reliability at high Angles: Given its just discussed constructional issues, the model is able to simulate a portion of the real condition well only for small closing angles. Infact, as it can be percieved in pictures like Figure 5.11 here proposed again, the absence of progressive accomodation of the channel shape (fixed side GVs, fixed walls) doesn' t allow a proper flow distribution, slowing down the right forth part of the flow and forcing the rear left to an exessive trajectory bending. This may eventually come out as a variation in the leakage vortex position, that pushed by a faster right flow may come closer to the suction side.

Eventually it can be said that the model regardless from its purpose, that might be corresponding to its real operation, is only useful to highlight and give a first idea of the leakage vortex dimensions as well as of the entity of the involved areas, pressure and velocities.

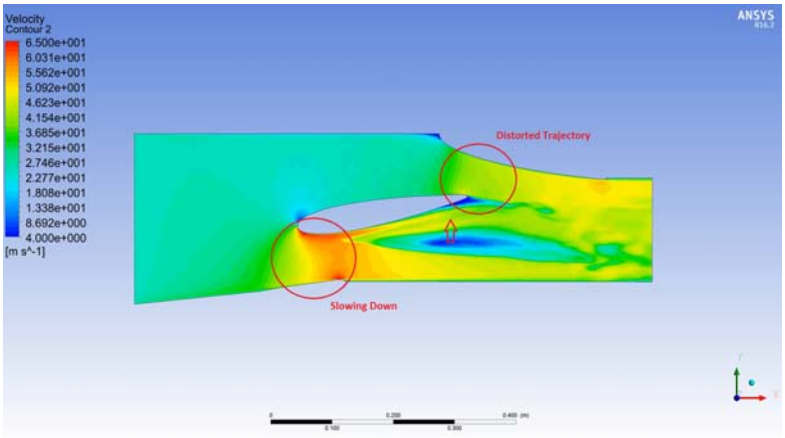

Figure 6.2: Weak points at high angles

6.2 Further Work

Finally some suggestions to be applied in the potential further works.
Another model should be built: it includes more blades (as shown in the example of the document [1] that featured 5 of them) to blend and reduce the side effects; then only the central profile should be supervised for data acquisition. Speaking of the inlet and outlet section, they should be shaped following the free vortex rule, in order to create an uniform and reliable flow field at the GV inlet section and keep the outlet condition the same at the Runner inlet. Hence, a CFD based optimization rested on the same free vortex condition ($R\ c_u = cost$), should be applied to redesign the walls that embed the side GV. From the cascade inlet to Guide Vanes inlet and from Runner inlet to the Cascade outlet, the channel should be shaped to develop the necessary flow conditions from axial flow to annular conditions and otherwise. More measurement section should also be pre arranged, especially in the Gap span, the most sensitive region computationally speaking, where the flow undergoes strong acceleration and high pressure gradients. It would eventually turn good if there is an interest also for the leaked mass flow in the gap.

Measurement sections: Several measurement sections should be prearranged. The most relevant levity committed by the previous model was to arrange only flat measurement section, (along with a flat inlet) that cant provide sure data exploitable also in a real machine simulation. So the potential new model should encounter these requirement by having at least GV inlet and Runner inlet sections that are shaped like those of the real machine. Infact CFX-Experimental data comparison, which are the reliability base on with every other further elaboration is built -such flow factor and gap clearance vortex development - can only be made strictly referring to the values (Velocity pressure ecc) taken in the same points, in the experimental model as well as in the Simulated one.

The Gap should also feature the shroud, that is neglected in the simulation, and all the blades (at least three, to take in account the cross effects rising from the interaction of the flow structure cropping out from each profile, plus two side blades embedded in the walls that can be fixed in both angle and Gap=0) should have the same gap and inclination towards the flow. Furthermore, aiming to enhance the model reliability and tightness to reality, a more

complex inlet section should be arranged, shaped in a manner to simulate the operational GV inlet condition, foreseeing the uneven velocity distribution due to both the vortex structure of the spiral casing and the stay vane wakes and related turbulence.

6.3 Final Considerations

At the very end it is convenient to sketch a general sum up of all the work done, by a recapitulation of all the relevant information acquired during this work employing the model.

- The presence of the clearance Gap heavily influences the velocity and pressure field, by changing its structure through the development of the leakage vortex, arising from the suction side and then propagating till the runner inlet and further.
- For low closing angles the model is valiant for the portion of the real flow field it replyes, naturally once the disturbance effects of the interation between the flow and the walls have been excluded.
- At low angles whichever the Gap may be Transient simulations aren' t necessary; the SS simulations are able alone to describe the developing of the system. At high angles the SS simulations lose every reliability handing over their task to the Transient ones.
- For high closing angles, even the model pulls itself ahead of the real situation, providing a distorted depiction of the Rear wake and leakage flow direction
- The resemblance between the SS simulated data and the experimental ones is satisfactory for every Gap span but loses its tightness as the closing angle increases.
- The turbulence is strongly dependent only from increased closing angles, whereas the Gap, even deeply changing the flow structure, doesn' t introduce much turbulence in the flow field.
- The turbulent flow starts off at nearly 4 Degrees from the maximum efficiency position.
- It has been understood that this model is worth to be considered the first step of a more detailed investigation, whose following phase is the construction and testing of a 5 profile model.

This work is intended to be a solid base towards a better understanding of the phenomenon of leakage flow through a Guide Vanes operational Gap.

Bibliography

[1] O.Univ.Prof.Dr.H.-B.Matthias
Analyse der Stromung und der Verluste im Leitschaufelbereich von Francisturbinen Institut fur Wasserkraftmaschinen und Pumpen; Wien, im Dezember 1996.

[2] I.B. Celik, U. Ghia, P.J. Roache, C.J. Freitas, H. Coleman, P.E. Raad
Procedure for Estimation and Reporting of Uncertainty due to Discretization in CFD Applications Journal of Fluids Engineering, `http://fluidsengineering.asmedigitalcollection.asme.org`

[3] Courant, R.; Friedrichs, K.; Lewy, H. *On the partial difference equations of mathematical physics*,(September 1956) [1928], AEC Research and Development Report, NYO-7689, New York: AEC Computing and Applied Mathematics Centre Courant Institute of Mathematical Sciences

[4] L.F. Richardson
The approximate aritmetical solution by Finite differences of Physical problems involving differential equations, with an application to the stresses in a Masonary dam Philos. Trans. R. Soc. London, Ser. A, 210, pp. 307-357.

[5] B.S. Thapa, O.G. Dahlhaug *Velocity and Pressure Measurements in Guide Vane clearance Gap of a low specific speed Francis Turbine*

[6] R. Koirala, B. Zhu, H.P. Neopane
Effect of the Guide Vane Clearance Gap on Francis Turbine performance www.mdpi/journal/energies

[7] R. Mack, P. Drtina, E. Lang
Numerical prediction of erosion on guide vanes and in labyrinth seals in hydraulic Turbines Sulzer Innotec, Winterthur 8401, Switzerland.

[8] Various Authors
Renewables 2016 Global Report

[9] W. Zhao, J.T. Billdal, T.K. Nielsen, H. Brekke
Study on the leakage flow through a clearance Gap between two stationary Walls 26th IAHR Symposium on Hydraulic Machinery and Systems; IOP Conf. Series: Earth and Environmental Science 15 (2012) 022015

[10] J. Bergmann-Paulsen
FSI - Analysis of a Francis Turbine NTNU - Norvegian University of Science and Technology, 2012

[11] H. Brekke
A discussion on losses, dynamic behaviour and cavitation on Francis Turbine Norwegian University of Science and Technology, Division of Thermal Energy and Hydropower, 2000

[12] O.G. Dahlhaug, B. Thapa
Sand erosion in a Francis Turbine - a case study from Jhimruk power plant, Nepal Norvegian University of Science and Technology NTNU, Trodheim, Norway

[13] S. Eide, H. Brekke
Analysis of the head covers deflection and the leakage flow in the Guide Vanes Norvegian University of Science and Technology NTNU, Trodheim, Norway, 2004

[14] S. Eide, O.G. Dahlhaug
Analysis of the leakage flow and wear in Guide Vanes Proceedings of the XXIst IAHR Symposium on Hydraulic Machinery and Systems September 9 - 12, 2002, Lausanne

[15] M. Eltvik, B.S. Thapa, O.G. Dahlhlaug
Numerical analysis of effect of design parameters and sediment erosion on a Francis runner ASIA-2012, March 26-27, Int. J. Hydropower and Dams, Chiang Mai, Thailand

[16] R. Guillaume, J-H. Deniau, D. Scolaro, C. Colombet
Influence of the rotor-stator interaction on the dynamic stresses of Francis runners Hydraulic Department of the Alstom Hydro Technology Center,82 av. Leon Blum, Grenoble, 38041, France; Mecanical Department of the Alstom Hydro Technology Center,82 av. Leon Blum, Grenoble, 38041, France

[17] R. Huang, B. Ji, X. Luo, Y. Zheng
Influence of Guide Vane shapes on hydraulic characteristics for a shaft-extension tubolar pump at Turbine mode Proceedings of the ASME 2014 4th Joint US-European Fluids Engineering Division Summer Meeting, FEDSM2014, August 3-7, 2014, Chicago, Illinois, USA

[18] Y.H. Jung, Y.U. Min, J.Y. Kim
Effect of tip clearance on suction performance at different flow rates in a mixed flow pump Proceedings of the ASME 2014 4th Joint US-European Fluids Engineering Division Summer Meeting, FEDSM2014, August 3-7, 2014, Chicago, Illinois, USA

[19] M. Kudo, K. Nishibe, M. Takahashi, K. Sato, Y. Tsujimoto
Study on Flow Characteristics Downstream of Annular Inlet Guide Vanes Proceedings of the ASME 2013 Fluids Engineering Division Summer Meeting, FEDSM2013, July 7-11, 2013, Incline Village, Nevada, USA

[20] W. Liao, J. Li
Numerical simulation and experimental investigation of the flow in end clearance region of the Guide Vane row of hydraulic Turbine Proceedings of the XXIst IAHR Symposium on Hydraulic Machinery and Systems, September 9 - 12, 2002, Lausanne

[21] F. Loiseau, M. Couston, M. Sabourin, J. Kirejczyk
Minimum Gap Guide Vane 22nd IAHR Symposium on hydraulic Machinery and Systems June 29 - July 2, 2004 Stockolm - Sweden

[22] P. Maruzewski, H. Hayashi, C. Munch, K. Yamaishi, T. Hashii, H.P. Mombelli, Y. Sugow, F. Avellan
Turbulence modeling for Francis Turbine water passages simulation 25th IAHR Symposium on Hydraulic Machinery and Systems

[23] K. Miyagawa, S. Fukao, Y. Kawata
Study on Stay Vane instability due to vortex shedding 22nd IAHR Symposium on Hydraulic Machinery and Systems June 29 - July 2, 2004 Stockholm - Sweden

[24] G.J. Peng, Y.Y. Luo, H.W. Fang, L.M. Zhai, Z.W. Wang
Study on the wearing law of the runner and Guide Vanes for a Francis Turbine Yangtze Delta Region Institute of Tsinghua University Zhejiang, Jiaxing, 314050, China

[25] S. Chitrakar, B.S. Thapa, O.G.Dahlhaug, H.P.Neopane
Numerical investigation of the flow phenomena around a low specific speed Francis turbine's Guide Vane cascade 28th IAHR Symposium on Hydraulic Machinery and Systems

[26] F.X. Shi, J.H. Yang, X.H. Wang, R.H. Zhang, C.E. Li *The impact of inlet angle and outlet angle of guide vane on pump in reversal based hydraulic turbine performance* School of Energy and Power Engineering, Lanzhou University of technology, GanSu, Lanzhou,730050, P.R.China

[27] P. Svaceka, M. Feistauerb, J. Horacekc
Numerical simulation of flow induced airfoil vibrations with large amplitudes Journal of Fluids and Structures 23 (2007) 391411

[28] C. Trivedi, B. Gandhi, C.J. Michel
Effect of transients on Francis turbine runner life: a review Journal of Hydraulic Research, 51:2, 121-132

[29] T.C. Vu, B. Nennemann, P. Ausoni, M. Farhat, F. Avellan
Unsteady CFD prediction of von Krmn vortex shedding in hydraulic turbine stay vanes cole Polytechnique Fdrale de Lausanne (EPFL)

[30] Y.X. Xiao, D.G. Sun, Z.W.Wang, J. Zhang, G.Y. Peng
Numerical analysis of unsteady flow behaviour and pressure pulsation in pump turbine with misaligned guide vanes State Key Laboratory of Hydroscience and Engineering and Department of Thermal Engineering, Tsinghua University, Haidian District, Beijing, 100084, China

[31] D. You, M. Wang, P. Moin, R. Mittal
Vortex Dynamics and Low-Pressure Fluctuations in the Tip-Clearance Flow Center for Turbulence Research, Stanford University

[32] W.G. Zhao, Y.B. Li, X.Y. Wang, J.P. Sun,G.X. Wu
Research on the effect of wear-ring clearances to the performance of centrifugal pump School of Energy and Power Engineering, Lanzhou University of Technology, Lanzhou, Gansu 730050, China

[33] V.Y. Karelin and C.G. Duan
Design of hydraulic machinery working in sand laden water, volume 2 Imperial College press, London, 1. edition edition, 2002.

[34] E. Bardal
Korrosjon og korrosjonsvern Tapir Forlag, NTH, Trondheim, 1. edition, 1985. ISBN 82-519-0700-4.

Thesis Consulted:

[35] Jonas Bergmann-Paulsen
FSI analysis of a Francis Turbine
Supervisor: Ole Gunnar Dahlhaug, EPT
Norwegian University of Science and Technology, Department of Energy and Process Engineering

[36] Arthur Tristan Favrel
Dynamics of the cavitation precessing vortex rope for Francis turbines at part load operating conditions
Supervisor: Prof. D. Pioletti, Ecole Politecnique Federal de Lausanne, Suisse 2016

[37] Peter Joachim Gogstad
Hydraulic design of Francis turbine exposed to sediment erosion
Supervisor: Ole Gunnar Dahlhaug, EPT
Norwegian University of Science and Technology, Department of Energy and Process Engineering, January 2012

[38] Christian Landry
Hydroacoustic Modeling of a Cavitation Vortex Rope for a Francis Turbine
FACULT DES SCIENCES ET TECHNIQUES DE L'INGNIEUR LABORATOIRE DE MACHINES HYDRAULIQUES PROGRAMME DOCTORAL EN ENERGIE, Ecole Politecnique Federal de Lausanne distitni slauti, Suisse, April 2015

[39] Chiragkumar Trivedi
Transients in High Head Francis Turbines Division of Fluid and Experimental Mechanics, Department of Engineering Sciences and Mathematics, Lule University of Technology, 971 87 Lule, Sweden, www.ltu.se

[40] O.O. Forde
Analysis of the Turbulent Energy Dissipation Master of Science in Product Design and Manufacturing, Norwegian University of Science and Technology, June 2012